



저작자표시-비영리-변경금지 2.0 대한민국

이용자는 아래의 조건을 따르는 경우에 한하여 자유롭게

- 이 저작물을 복제, 배포, 전송, 전시, 공연 및 방송할 수 있습니다.

다음과 같은 조건을 따라야 합니다:



저작자표시. 귀하는 원저작자를 표시하여야 합니다.



비영리. 귀하는 이 저작물을 영리 목적으로 이용할 수 없습니다.



변경금지. 귀하는 이 저작물을 개작, 변형 또는 가공할 수 없습니다.

- 귀하는, 이 저작물의 재이용이나 배포의 경우, 이 저작물에 적용된 이용허락조건을 명확하게 나타내어야 합니다.
- 저작권자로부터 별도의 허가를 받으면 이러한 조건들은 적용되지 않습니다.

저작권법에 따른 이용자의 권리는 위의 내용에 의하여 영향을 받지 않습니다.

이것은 [이용허락규약\(Legal Code\)](#)을 이해하기 쉽게 요약한 것입니다.

[Disclaimer](#)

Master of Science

**IMPROVED TRIBOLOGICAL PERFORMANCE OF MOS₂
USING MULTIWALLED CARBON NANOTUBES**

The Graduate School
of the University of Ulsan
Department of Mechanical Engineering
Duy Thanh Le

**IMPROVED TRIBOLOGICAL PERFORMANCE OF MOS₂
USING MULTIWALLED CARBON NANOTUBES**

Supervisor: Professor Koo-Hyun Chung

A Dissertation

Submitted to

the Graduate School of the University of Ulsan

In partial Fulfillment of the Requirements

for the Degree of

Master of Science

by

Duy Thanh Le

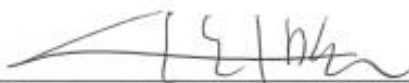
Department of Mechanical Engineering

University of Ulsan, Korea

August 2023

**IMPROVED TRIBOLOGICAL PERFORMANCE OF MOS₂
USING MULTIWALLED CARBON NANOTUBES**

This certifies that the master's thesis
of Le Thanh Duy is approved.



Committee Chair Professor. Chun Doo-Man



Committee Member Professor. Chung Koo-Hyun



Committee Member Professor. Hong Sung Tae

Department of Mechanical Engineering
University of Ulsan, Korea
August 2023

ACKNOWLEDGEMENT

I would like to express my deepest gratitude to my thesis advisor, Professor Koo-Hyun Chung, for his invaluable guidance, support, and encouragement throughout the course of this research. His expertise, constructive criticism, and insightful feedback have been instrumental in shaping my work and helping me achieve my academic goals. I am truly fortunate to have had the opportunity to work with him and will always cherish the knowledge and skills I gained under his supervision.

I would also like to extend my heartfelt thanks to my labmates, for their companionship, friendship, and collaboration during this journey. Their willingness to share their ideas, expertise, and resources has been crucial in making this research possible. I have learned so much from their diverse backgrounds and perspectives, and I am grateful for the memories we have shared both inside and outside the lab.

Furthermore, I would like to acknowledge the staff and faculty members of the Department of mechanical engineering, whose dedication to education and research has created an inspiring and supportive environment for me to pursue my academic aspirations. Their contributions to the field and commitment to excellence have set a high standard for me to follow in my future endeavors.

Finally, I would like to thank my family and friends for their unwavering love, encouragement, and support throughout my academic journey. Their belief in me and their sacrifices have been the driving force behind my achievements, and I owe them a debt of gratitude that I can never fully repay.

Thank you all for your contributions to this thesis and for enriching my life in countless ways.

TABLE OF CONTENTS

| | |
|--|--------|
| ACKNOWLEDGEMENT | i |
| TABLE OF CONTENTS | ii |
| LIST OF FIGURES | iv |
| ABSTRACT | vii |
| 1. INTRODUCTION..... | - 1 - |
| 1.1. Background and motivation..... | - 1 - |
| 1.2. Objective of the thesis | - 6 - |
| 2. EXPERIMENTAL DETAILS | - 7 - |
| 2.1. Fabrication of MoS ₂ Nanoflakes | - 7 - |
| 2.2. Preparation of CNT matrix substrate..... | - 9 - |
| 2.3. Layer Transfer of MoS ₂ | - 11 - |
| 2.4. Raman Spectra Analysis | - 12 - |
| 3. FRICTION CHARACTERISTICS OF MOS ₂ /CNT..... | - 14 - |
| 3.1. The friction of MoS ₂ supported on CNT matrix, PMMA, and Si/SiO ₂ | - 14 - |
| 3.2. The effect of density of CNT matrix | - 17 - |
| 3.3. The effect of suspended MoS ₂ | - 21 - |
| 3.4. The effect of MoS ₂ thickness | - 25 - |
| 3.5. The effect of CNT orientation..... | - 28 - |
| 4. CONCLUSIONS AND RECOMMENDATIONS | - 36 - |
| 4.1. Conclusions..... | - 36 - |

4.2. Recommendation for future works..... - 38 -

REFERENCES - 39 -

LIST OF FIGURES

| | |
|---|--------|
| Figure 1. 1 Three-dimensional representation of the structure of MoS ₂ : single layer, 0.65nm thick, can be extracted using scotch tape-based micromechanical cleavage; (b) optimized structures of the MoS ₂ monolayer with four adsorption sites: (1) hollow site, (2) top site of the S atom, (3) Mo–S bridge site, and (4) top site of the Mo atom [31]..... | - 2 - |
| Figure 1. 2 Schematic representation of single walled carbon nanotube (SWCNT) and multi walled carbon nanotube (MWCNT) [32] | - 4 - |
| Figure 2. 1 Optical microscopy image of atomically thin MoS ₂ specimen..... | - 8 - |
| Figure 2. 2 AFM friction loop | - 8 - |
| Figure 2. 3 Schematic illustration of preparation of CNT matrix substrate | - 10 - |
| Figure 2. 4 The figure displays the AFM topography images of MWCNTs on a SiO ₂ /Si substrate. The initial volume of the CNT solution used was 300 µl: Before and After Transfer Process..... | - 10 - |
| Figure 2. 5 Schematic illustration of the transfer process of MoS ₂ over CNT matrix substrates. (a) Mechanically exfoliated MoS ₂ flake on SiO ₂ /Si substrate. (b) A spin-coated PMMA support layer is on the MoS ₂ . (c) The stack is immersed in 1 M NaOH solution at 80 °C. The PMMA/MoS ₂ stack is then detached from the substrate within few mins. (d) A spin-coated CNT is on the Si/SiO ₂ . (e) The detached PMMA/MoS ₂ stack is transferred onto CNT matrix substrate. (f) In the final step, the post-transferred PMMA was removed by hot acetone. | - 12 - |
| Figure 3. 1 Friction force as a function of normal force with different substrates with a MoS ₂ thickness of 1L (~ 0.9nm). (a) (b) AFM topographic images of MoS ₂ before and after transferring onto CNT matrix (c) FFM (forward scan) images of MoS ₂ at 20nN normal force. (d) variations in friction force of the MoS ₂ on PMMA, CNT matrix and Si/SiO ₂ for 1L with respect to the normal force. (e) Raman spectra and E _{2g} ¹ and A _{1g} . In (a)-(c), the red dashed lines | |

indicate the locations where the cross-sectional profiles, and friction loops were taken. - 15

Figure 3. 2 Friction force as a function of normal force with different E of CNT matrix with a MoS₂ thickness of 2L (~ 1.5nm). (a) AFM topographic images of MoS₂ before and after transferring onto CNT matrix (b) FFM (forward scan) images of MoS₂ at 20nN normal force. (c) variations in friction force of the MoS₂ on CNT matrix and Si/SiO₂ for 2L with respect to the normal force. In (a)-(b), the red dashed lines indicate the locations where the cross-sectional profiles, and friction loops were taken. - 19 -

Figure 3. 3 (a) Raman spectra of the studied samples obtained at room temperature using 532 nm wavelength laser. (b) Raman spectrum of Si/SiO₂ of 4 specimens. The inset (c) shows the Raman spectrum of CNT on Si/SiO₂ substrate obtained at room temperature with the same laser excitation. - 20 -

Figure 3. 4 Friction force as a function of normal force with different suspended MoS₂ thickness (a) (b) AFM topographic images of MoS₂ before and after transferring onto CNT matrix (c) FFM (forward scan) images of suspended MoS₂ on CNT fiber at 20nN normal force. The inset (c) shows the topography images of measured areas. Raman spectra and E_{2g}¹ and A_{1g}. In (a)-(c)-(d), the red dashed lines indicate the locations where the cross-sectional profiles, and friction loops were taken..... - 23 -

Figure 3. 5 Frictional forces for suspended MoS₂ on CNT for 2L, 3L, 4L MoS₂ with respect to the normal force. - 24 -

Figure 3. 6 (a) AFM topographic images, (b) FFM (forward scan) images of MoS₂ at 20nN normal force, and (c) variations in friction force of the MoS₂ on CNT matrix for 1L, 2L, 3L, 4L MoS₂ with respect to the normal force. In (a)-(b), the red dashed lines indicate the locations where the cross-sectional profiles, and friction loops were taken. - 26 -

Figure 3. 7 (a) AFM topographic images of MoS₂ onto CNT matrix. Friction images of the normal orientation (b) and after rotating the specimen of 90 degrees (c). (d) variations in friction force of the MoS₂ on CNT matrix for different sliding motion with respect to the normal force. The red dashed lines indicate the locations where the cross-sectional profiles, and friction loops were taken. The friction force profile (red solid line) is the average profile inside the area delimited by the dotted line in b,c..... - 28 -

Figure 3. 8 (a),(b) AFM topographic images of MoS₂ before and after transferring onto CNT matrix. Friction images of the highlighted transverse (c) and longitudinal (d). The red dashed lines indicate the locations where the cross-sectional profiles, and friction loops were taken. The friction force profile (red solid line) is the average profile inside the area delimited by the dotted line in c,d..... - 30 -

Figure 3. 9 (a)-(c) Anisotropy ratio of friction on MoS₂ with different thicknesses. (d) The friction ratio as a function of normal load on MoS₂ different thicknesses..... - 31 -

Figure 3. 10. Frictional forces for transverse and longitudinal sliding - 33 -

ABSTRACT

Improved Tribological Performance of MoS₂ Using Multiwalled Carbon Nanotubes

Duy Thanh Le

School of Mechanical Engineering

The Graduate School

University of Ulsan

Molybdenum disulfide (MoS₂) and other two-dimensional (2D) materials like phosphorene, graphene, hexagonal boron nitride, and transition metal dichalcogenides (TMDCs) are attracting huge attention in both academia and industry due to their outstanding optical and electrical properties. TMDCs have opened up a new field of science of 2D layered materials and provided a widespread field for exploration of physics at the nanoscale. Based on the presence of the bandgap or the strong ambipolar electric effect, single and a few layers MoS₂ and graphene have a great potential in micro- and nano-electromechanical systems (MEMS and NEMS). Furthermore, due to the low friction characteristics of MoS₂ and graphite, they may have a great potential as a protective layer in MEMS and NEMS applications.

Since the discovery of carbon nanotubes (CNTs), they have strongly attracted attention because of their unique electrical, optical, and mechanical properties. For example, the electrical properties vary from semiconductor to conductor, and the mechanical properties show high tensile strength with flexibility.

Recent advances in nanomaterials have provided new opportunities for achieving extremely low wear. Nanomaterials have already demonstrated their ability to reduce wear at

the macro-scale. The combination of different layers, including interlayers, in a multilayer coating can provide additional benefits due to their synergistic effects. The improvement of friction and wear properties of a surface with a multilayer coating depends on factors such as the type of coating, the thickness of individual layers, and the number and order of layers. Even with just two well-designed layers, a significant reduction in friction and wear can be achieved. Fabricating a coating with a multilayer structure is a viable wear-reduction strategy that can be readily adopted owing to recent advances in deposition technology. By incorporating soft a-C layers in between hard a-C layers, high hardness-to-elastic modulus ratio can be attained. This helps alleviate residual stress throughout the coating, making elasticity a crucial factor in mitigating coating wear.

Several studies have explored the use of nanomaterials, including carbon nanotubes (CNTs) and PMMA, to enhance the elasticity and damping effects of wear-resistant coatings. To minimize surface wear, multiple mechanical characteristics must be controlled simultaneously, which can be achieved through the design of a nanostructured surface. However, there is currently a lack of comprehensive studies on the tribological behavior of 2D materials on these materials, and the existing literature provides limited information on the effects of the elasticity of CNT on their friction behavior. Therefore, conducting a systematic investigation of the tribological properties will contribute to the scientific understanding of these materials and advance the development of their potential applications. The study will contribute to the scientific understanding of the tribological behavior of MoS₂/CNT for improved wear resistance and lubrication to gain a better understanding of the relationship between elasticity and tribological performance in these materials. Specifically, the aim is to identify how changes in elasticity impact the friction and wear behavior of MoS₂/CNT and to investigate the underlying mechanisms responsible for these effects. The friction reduction mechanism of the CNT matrix was investigated using AFM to precisely measure friction force.

1. INTRODUCTION

1.1. Background and motivation

The discovery of graphene raised the excitement over two dimensional atomically layered materials, which have distinct properties from their bulk counterparts due to quantum confinement. Two-dimensional (2-D) crystal, including single- and a few atomic layers of MoS₂ and graphene, have attracted a lot of interest for fundamental studies due to their remarkable electrical properties. Their atomic scale thickness and planar geometry makes themselves interesting for MEMS and NEMS application where they can exhibit fascinating properties. Recently, the discovery of graphene by using the micromechanical exfoliation of graphite has received great interest due to its unique properties [1, 2]. There are many notable properties, which have been discovered through the investigation of pristine graphene such as extremely high charge of electrons and holes mobility ($\sim 230,000 \text{ cm}^2/\text{Vs}$), high thermal conductivity ($\sim 3000 \text{ W/mK}$), the ultimate strength ($\sim 130 \text{ GPa}$) [3-5]. Due to the combination of these fascinating electrical, mechanical, thermal and chemical properties, graphene has received significant attention as a novel material for electrical applications [3-5]. However, graphene's still limited at some given electrical application such as high-speed analog electronics due to the lack of intrinsic bandgap [6].

Atomically thin MoS₂, which is also a graphene-like two-dimensional material, has received enormous attention due to its striking optical, electronic, and mechanical properties. [3–5] Single-layer MoS₂ has a direct optical gap of 1.8 eV. [6–8] The presence of this band gap makes MoS₂ interesting for applications in nanoelectronics where it allows the fabrication of transistors with low power dissipation and current on/off ratios. The applications of MoS₂ also include the field-effect transistors (FET), [9,10] valleytronics, [11–16] phototransistors, [17,18] gas sensors, [19] catalytic hydrodesulfonation, [20,21] hydrogen evolution, [22,23]

photoelectrochemical hydrogen production, [24–27] small-signal amplifiers, [28] solid lubricants, [29] and nonvolatile memory cells. [30]

Another interest of MoS₂ and graphite is the low friction characteristics. Conventionally, bulk MoS₂ and graphite have been proposed as a solid lubricant due their low friction characteristic. MoS₂ and graphite with a layered structure have a weak interlayer bonding, and therefore the shear strength at contacting interface may be relatively low, which in turn allows low friction characteristics.

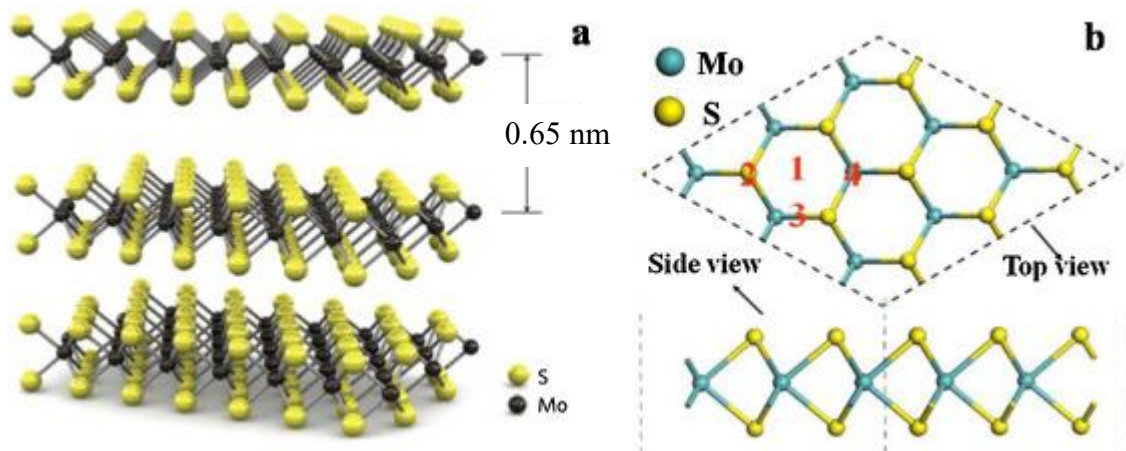


Figure 1. 1 Three-dimensional representation of the structure of MoS₂: single layer, 0.65nm thick, can be extracted using scotch tape-based micromechanical cleavage; (b) optimized structures of the MoS₂ monolayer with four adsorption sites: (1) hollow site, (2) top site of the S atom, (3) Mo–S bridge site, and (4) top site of the Mo atom [31]

Over several decades, numerous studies have been conducted to reduce mechanical system wear. The hardness of a material is one of the most important mechanical properties in wear and is widely used to determine abrasive wear resistance. While some annealed pure metals and steels exhibit linearly proportional abrasive wear resistance with increasing hardness, there are cases where the abrasive wear resistance remains unchanged or even decreases despite considerable hardness increases through work hardening or heat treatment. Moore's study shows that the effects of hardness and microstructure on abrasive wear differ between steel types, with microstructure having a greater influence on abrasive wear resistance than bulk

hardness for ferritic steels. Hard anodized coatings also demonstrate that wear rate is not directly related to hardness. Thus, a higher hardness does not always guarantee a better abrasive wear resistance, and additional strategies are needed for designing wear-resistive surfaces beyond simply enhancing hardness. These findings highlight the need to consider other factors besides hardness in assessing abrasive wear resistance.

Fabricating a coating with a multilayer structure is a viable wear-reduction strategy that can be readily adopted owing to recent advances in deposition technology. A high hardness to elastic modulus ratio can be achieved by inserting soft a-C layers between the hard a-C layers, which relieves the residual stress of the entire coating. Therefore, the elasticity of the coating is critical for reducing coating wear.

MWCNTs discovered in 1991 have been widely used as fillers to enhance the mechanical and tribological properties of polymer matrix composites. Owing to their unique structure, superb mechanical, electrical, and chemical characteristics, such as high tensile strength and elastic modulus along the longitudinal direction, and good elastic and thermal conductivity properties. Based on these unique properties, various CNT applications have been suggested, such as probe tips for atomic force microscopy (AFM) and scanning tunneling microscopy (STM), rotational actuators, field emission devices, electric motor brushes, and chemical sensors. Owing to their small dimensions, CNTs are regarded as suitable materials for exploitation in several precision industries such as semi-conductors, batteries, and display devices. Some researchers have also focused on the ability of the outstanding mechanical properties of CNTs to improve durability and tribological characteristics. There have been several attempts to exploit CNTs in reinforcing polymers or metal composites. The utilization of CNTs as additives in lubricants has also been considered by several researchers.

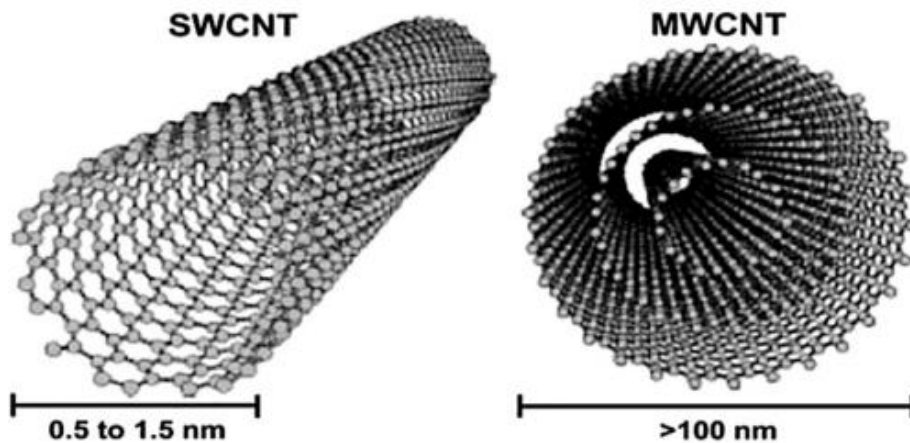


Figure 1. 2 Schematic representation of single walled carbon nanotube (SWCNT) and multi walled carbon nanotube (MWCNT) [32]

To provide enhanced elasticity or damping effects, a few studies have employed nanomaterials such as carbon nanotubes (CNTs) and fullerenes. The stiffness of a system can be controlled by designing a nanostructured surface. In the case of a properly designed nanostructured surface, the wear was noticeably reduced owing to elastic deformation and recovery of the nanostructure. This indicates that several mechanical characteristics should be controlled simultaneously to minimize surface wear depending on the contact sliding condition. According to the aforementioned literature survey, wear-resistant coatings should have excellent elasticity and capability to distribute contact stress to provide further wear resistance.

Therefore, nanostructured thin films composed of randomly aligned CNTs are expected to have low mechanical stiffness due to abundant voids between the nanotubes and resistance to permanent deformation owing to the superior mechanical strength of CNTs. However, there are still lacking studies on the structured film comprising CNTs with sufficient vacant space.

Many studies regarding composite coatings with CNT reinforcement reported tribological improvements because the interaction between fillers and reinforcements enhanced the mechanical properties of the entire coating. Thus, the strategy of this work is the opposite of

the aforementioned literature because a nanostructure composed of CNTs only was considered to supply voids inside, decreasing the hardness and elastic modulus.

To demonstrate the friction reduction mechanism of the CNT thin film, the AFM was used to conduct friction test.

1.2. Objective of the thesis

The objective of this thesis is firstly to achieve a fundamental knowledge of friction characteristics of MoS₂ on CNT matrix. Secondly, the study will contribute to the scientific understanding of the tribological behavior of MoS₂/CNT for improved wear resistance and lubrication to gain a better understanding of the relationship between elasticity and tribological performance in these materials. Specifically, the aim is to identify how changes in elasticity impact the friction and wear behavior of MoS₂/CNT and to investigate the underlying mechanisms responsible for these effects.

2. EXPERIMENTAL DETAILS

2.1. Fabrication of MoS₂ Nanoflakes

MoS₂ crystals were acquired from SPI Supplies Inc. and subsequently subjected to mechanical exfoliation to obtain MoS₂ layers, which were then deposited on Si substrates with a thermally grown oxide thickness of approximately 300 nm. The MoS₂ nanosheets were carefully examined using optical microscopy to ensure that they were devoid of any tape residue. The thickness of the MoS₂ layers was determined using an atomic force microscope (AFM, MFP-3D, Asylum Research) operated in tapping mode.

The AFM was also employed to obtain the topography of the MoS₂ layers, also in tapping mode, while the friction forces were measured using a calibrated AFM. It is noteworthy that the calibrated normal and lateral force sensitivities were varied for each set of experiments. The FFM images, including the stick-slip lattice, were analyzed with the scan direction being perpendicular to the cantilever body length direction.

Figure 2.1 shows a typical optical microscopy image of these exfoliated MoS₂ specimens consisting of single-layer (1L) and bi-layer (2L). Similar to graphene [27], based on the distinct optical contrast, the number of MoS₂ layers can be easily identified with a “naked eye” using an optical microscope.

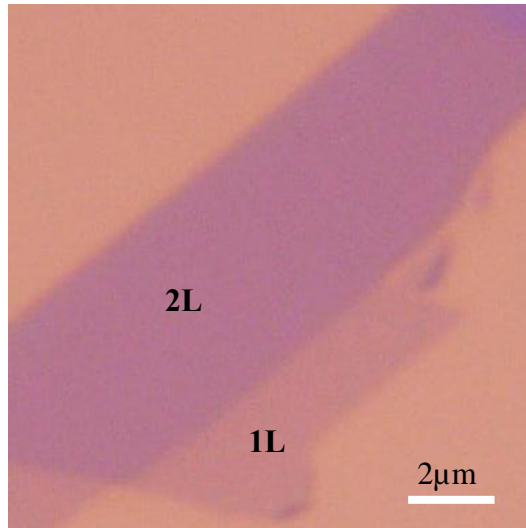


Figure 2. 1 Optical microscopy image of atomically thin MoS₂ specimen.

The number of MoS₂ layers was determined by the AFM (MFP-3D, Asylum Research) imaging. Considering that the thickness of these specimens may be more accurately determined by contact mode. For the high resolution topographic purpose, the intermediate imaging method was prefer than the contact imaging method due to the surface modification possibility of the specimens caused by the contact scanning between AFM tips and specimen's surfaces. The silicon AFM probes with a nominal spring constants of 2 N/m (AC240, Olympus) and 0.2 N/m (LFMR, Nanosensors) are used for intermediate contact and contact mode imaging, respectively.

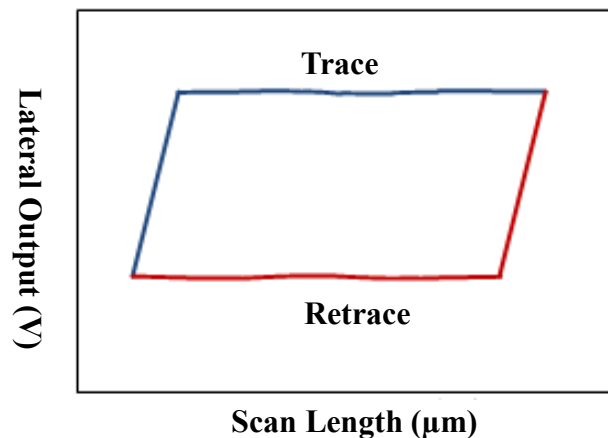


Figure 2. 2 AFM friction loop

Friction force microscopy (FFM) images were simultaneously obtained during contact mode imaging. For quantitative force measurement, the LFMR AFM probes are calibrated in both normal [33] and lateral [34] directions. The normal force in contact mode imaging is set to 0.5 nN in order to minimize the damage of both AFM probe [35, 36] and the specimen during the measurement. Furthermore, for the experimental consistency in the friction force measurement, the wear of the AFM probe was indirectly monitored from the variation of the adhesion force [37] which was determined by force-displacement curve before and after each FFM imaging. The friction force was calculated by dividing the difference between trace and retrace value of friction loop by two.

2.2. Preparation of CNT matrix substrate

The multi-walled carbon nanotubes (MWCNTs) were initially suspended in isopropyl alcohol (IPA) and agitated in an ultrasonic bath for approximately an hour. The solution's density was adjusted to achieve a slightly grayish appearance post-sonication. Subsequently, a droplet of the resulting solution was drop-casted onto an untreated, clean silicon wafer through spin coating at 6000 rpm. After 60 seconds of spin coating, any residual solution was eliminated by heating in. This process can be repeated several times to increase the CNT density on the surface. The MWCNTs will adhere to the silicon substrate and will be ready for transfer.

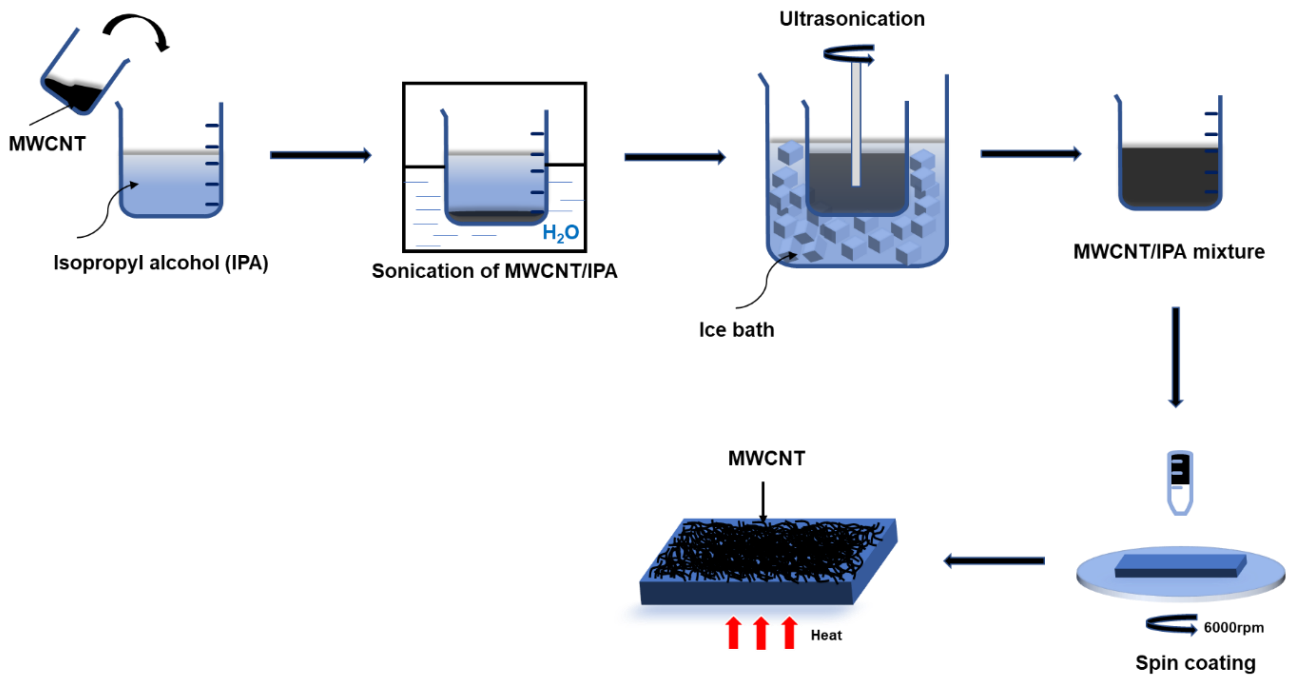


Figure 2. 3 Schematic illustration of preparation of CNT matrix substrate

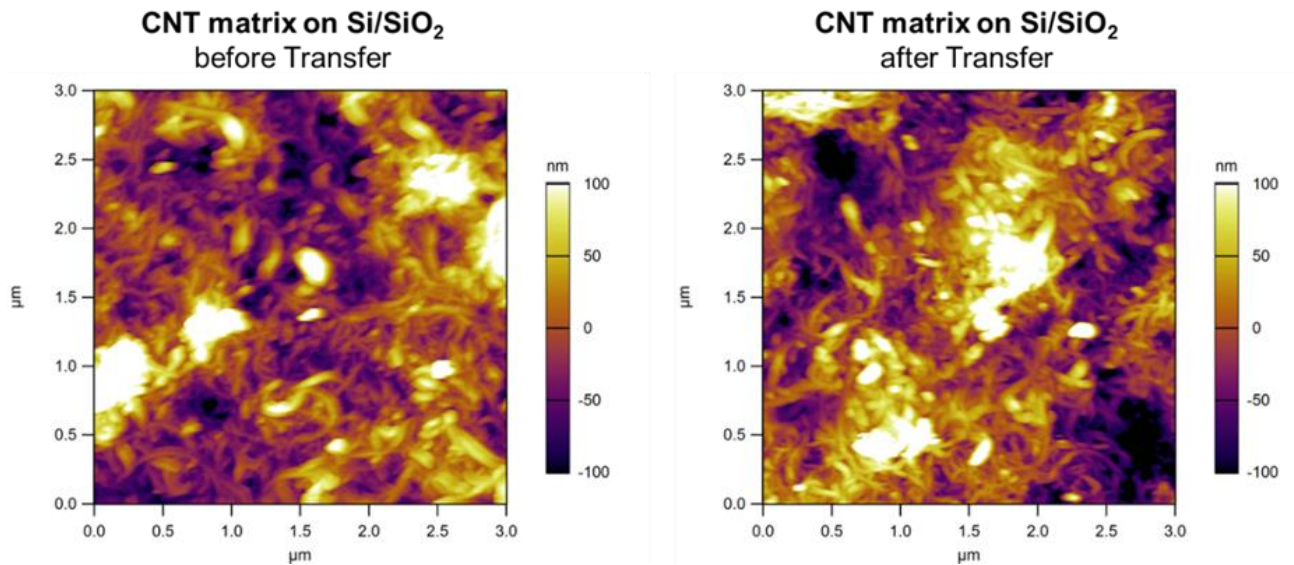


Figure 2. 4 The figure displays the AFM topography images of MWCNTs on a SiO₂/Si substrate. The initial volume of the CNT solution used was 300 μl: Before and After Transfer Process

The structural integrity of the CNT matrix was maintained after the transfer process, and the density of the matrix was preserved without any significant damage observed in Figure 2.3.

This finding suggests that the transfer process did not compromise the structural stability of the CNT matrix. The successful preservation of the CNT matrix density is crucial for applications that require a high density of CNTs. Furthermore, the absence of damage to the CNT matrix is beneficial since the structural integrity of the matrix plays a crucial role in its mechanical and electrical properties. Therefore, the transfer process used in this study is a promising technique for preserving the structural integrity of CNT matrices during transfer, enabling their use in various applications without compromising their properties.

2.3. Layer Transfer of MoS₂

A thin layer of PMMA was spin-coated onto exfoliated MoS₂ film/flakes at a speed of 3000 rpm for 60 s, and the assembly was left at room temperature overnight (Figure 2.4 a,b).. Subsequently, the PMMA/MoS₂ stack on the Si/SiO₂ wafer was placed in a beaker filled with 1 M NaOH solution. Prior to placing the stack in the beaker, one edge of the MoS₂ growth area was partially scratched using a blade so that the NaOH solution could penetrate at the interface of MoS₂ and the substrate, and the solution could dissolve the water-soluble layer of Na₂S/Na₂SO₄ underneath the MoS₂ flakes/film easily. The NaOH solution partially etches the surface of SiO₂, and the combined effect of partial etching of the SiO₂ surface and dissolution of the water-soluble layer causes the PMMA/MoS₂ stack to lift off and float on the NaOH surface (see Figure 2.4 c). The PMMA/MoS₂ film floating on the NaOH surface was then rinsed three times with DI water to remove any contaminants. After the rinse, the PMMA/MoS₂ stack was transferred onto the desired target substrate. The post-transferred PMMA/MoS₂/TS was dried by N₂ gas and left again overnight at room temperature for complete evaporation of water molecules and better adhesion of transferred MoS₂ flakes/film with the new substrate. The remaining PMMA polymer residues were removed by putting the transferred MoS₂ film in hot acetone for 4 hours at 100 °C. [38]

The surface morphology of both the as grown and transferred MoS₂ flakes was observed using an optical microscope (OM). The optical properties and thickness of the MoS₂ film before and after transfer were studied by Raman and photoluminescence spectroscopy. Atomic force microscopy (AFM) was used to study morphology.

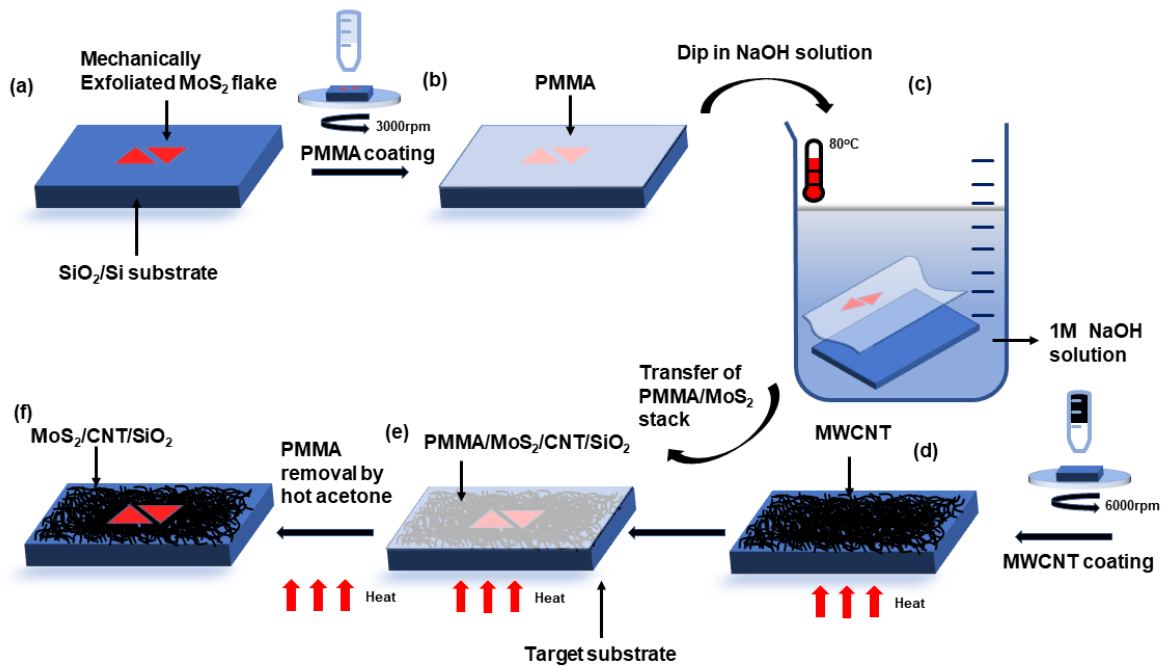


Figure 2. 5 Schematic illustration of the transfer process of MoS₂ over CNT matrix substrates. (a) Mechanically exfoliated MoS₂ flake on SiO₂/Si substrate. (b) A spin-coated PMMA support layer is on the MoS₂. (c) The stack is immersed in 1 M NaOH solution at 80 °C. The PMMA/ MoS₂ stack is then detached from the substrate within few mins. (d) A spin-coated CNT is on the Si/SiO₂. (e) The detached PMMA/MoS₂ stack is transferred onto CNT matrix substrate. (f) In the final step, the post-transferred PMMA was removed by hot acetone.

2.4. Raman Spectra Analysis

In order to characterize the thickness of these atomically thin specimens and the materials properties associated with the thickness, Raman spectroscopy has been widely utilized, owing

to the sensitivity of vibrational spectrum to the thickness [28, 29]. Raman spectra were obtained using Raman spectroscopy with an Ar⁺ laser (532 nm). The laser spot size was ~0.5 μm and far less than the desired areas that the laser beam can be exerted right on the part of MoS₂ on Si/SiO₂, CNT matrix, and PMMA. The laser power was ~2 mW and this could eliminate the local heating effect of a laser beam on the MoS₂ nanoflake. The accumulation time was 10 s and 3 cycles were adopted one time to ensure sufficient signal intensity. The temperature and relative humidity were at room temperature.

3. FRICTION CHARACTERISTICS OF MoS₂/CNT

Friction force measurement was conducted after the MoS₂/CNT specimen preparation. We quantitatively investigated friction force of MoS₂ on CNT with different set of experiments.

3.1. The friction of MoS₂ supported on CNT matrix, PMMA, and Si/SiO₂

In this section, the friction of MoS₂ supported on CNT matrix, PMMA, and Si/SiO₂ were systematically investigated using the Raman spectroscopy and atomic force microscopy (AFM). The specimens were measured with the different normal force. In particular, the effect of substrates is assessed by FFM. We found that the use of CNT matrix as a substrate may have other advantages, such as high mechanical strength, thermal conductivity, and electrical conductivity, which make it suitable for a variety of applications.

Topographic images of the atomically thin specimens obtained from intermittent-contact mode AFM using relatively sharp Si AFM tips with a nominal tip radius of around 2 nm, as shown in Figure 3.1 a, clearly demonstrate the relatively clean surfaces of these specimens. On the basis of the cross-sectional height profiles, single-layer MoS₂ thicknesses were determined to be about 0.9nm, in good agreement with previous studies. [39–41]

Single MoS₂ films were further examined by Raman spectroscopy with a 532 nm excitation source at room temperature. Raman spectra of atomically thin MoS₂ specimens, as shown in Figure 3.1 e, clearly show the dependence of their Raman characteristic peaks on the thickness, which is consistent with other studies. [42-44]. In the case of atomically thin MoS₂ specimens, their Raman spectra show two Raman characteristic peaks, the E_{2g}^1 and A_{1g} peaks, which are associated with the in-plane vibrations of Mo–S atoms and the out-of-plane vibration of S atoms, respectively.

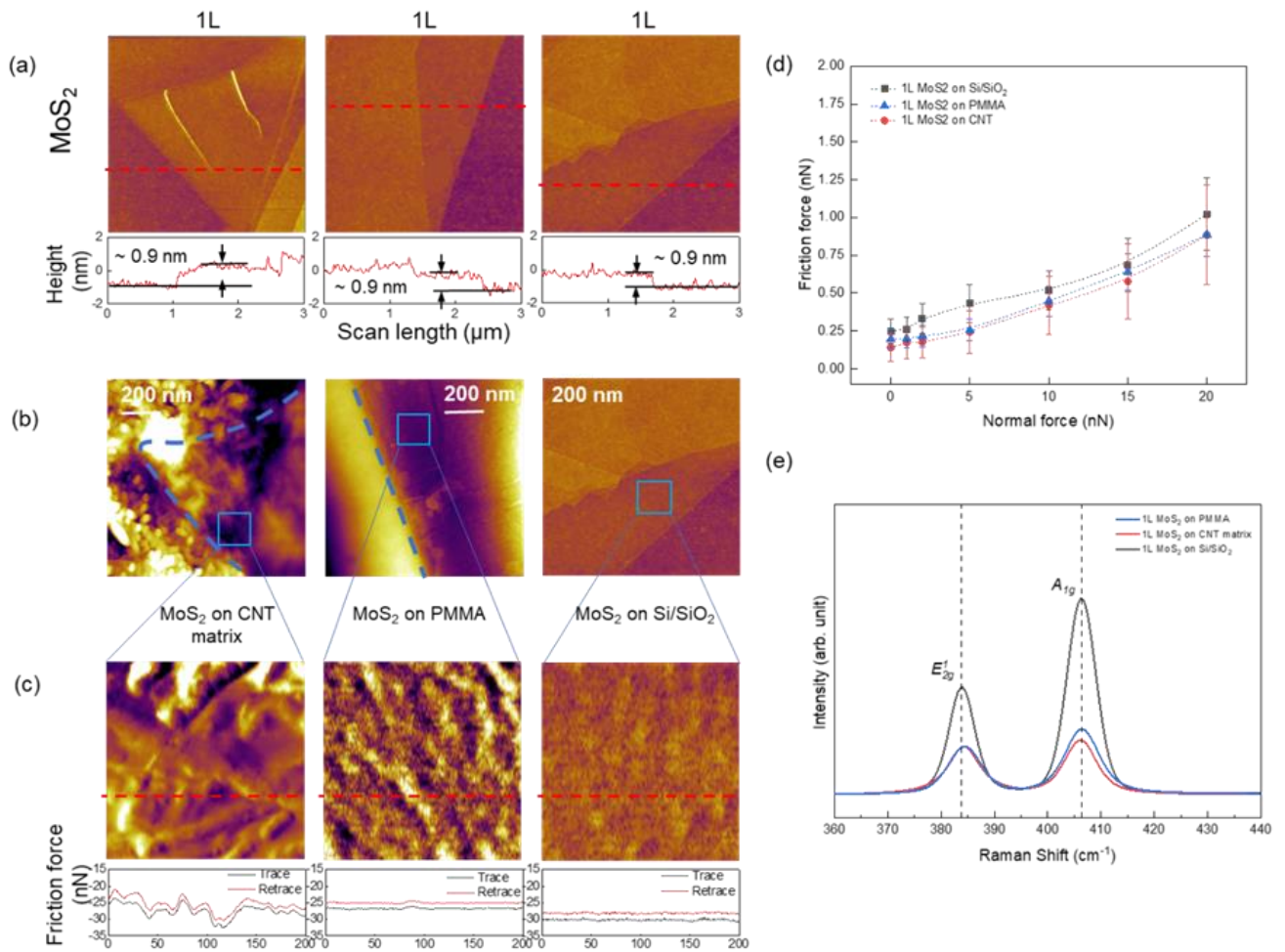


Figure 3. 1 Friction force as a function of normal force with different substrates with a MoS₂ thickness of 1L (~ 0.9nm). (a) (b) AFM topographic images of MoS₂ before and after transferring onto CNT matrix (c) FFM (forward scan) images of MoS₂ at 20nN normal force. (d) variations in friction force of the MoS₂ on PMMA, CNT matrix and Si/SiO₂ for 1L with respect to the normal force. (e) Raman spectra and E_{2g}¹ and A_{1g}. In (a)-(c), the red dashed lines indicate the locations where the cross-sectional profiles, and friction loops were taken.

After characterization of the thickness of atomically thin MoS₂ specimens on different substrates using AFM and Raman spectroscopy, friction forces were evaluated as function of normal force. In this test, friction force of single-layer MoS₂ on different substrates were

measured with a silicon AFM tip under normal forces ranging from 0 to 20 nN. The friction force variation with respect to normal force during the test was noted as shown in Figure 3.1 d. In addition, FFM images from only the forward scan directions were included for clarity, where the smaller friction loops indicate lower friction and larger one indicates higher friction.

The data on the friction coefficients of MoS₂ supported on CNT matrix, PMMA, and Si/SiO₂ provide valuable insights into the tribological properties of these materials. Our study found that the friction coefficient of MoS₂ on CNT matrix was lower than that on PMMA and Si/SiO₂, with values of 0.22, 0.33, and 0.17, respectively under 2nN. This suggests that the use of CNT matrix as a substrate may be advantageous in certain applications where a lower friction coefficient is desired.

There are several possible explanations for the lower friction coefficient observed on the CNT matrix substrate. CNTs have been shown to exhibit lower friction coefficients compared to PMMA and other polymers, due to their unique mechanical and tribological properties. CNTs have high aspect ratios, meaning that they have a large surface area to volume ratio, which can enhance their lubricating properties. Additionally, the smoothness of the CNT surface and the absence of chemical bonding between the CNT and the counterface can also contribute to their low friction behavior. [46]

The friction force between PMMA and CNT depends on various factors such as the conditions under which the friction force is being measured (e.g., temperature, humidity, load) [47], the type of CNT (single-walled or multi-walled), and the surface area of the CNT and PMMA in contact. However, it is important to note that the specific conditions and the type of CNT being used can still have a significant impact on the friction force and it is not always the case that CNTs will have lower friction than PMMA.

It is important to note that the lower friction coefficient observed on the CNT matrix substrate does not necessarily indicate inferior performance compared to the other substrates. In fact, in

some applications where low friction is desirable, the CNT matrix substrate may be the best choice. Additionally, the use of CNT matrix as a substrate may have other advantages, such as high mechanical strength, thermal conductivity, and electrical conductivity, which make it suitable for a variety of applications.

3.2. The effect of density of CNT matrix

On the basis of the friction force of MoS₂ on CNT matrix from previous tests, the CNT matrix substrate indicates superior performance compared to the other substrates. In general, the results show that the use of CNT matrix as a substrate may be advantageous in certain applications where a lower friction coefficient is desired. To gain a better understanding of the effect of CNT matrix, friction force tests were performed as a function of CNT density.

In the friction tests, an LFM tip was used to measure a defined area of 200 nm × 200 nm on the surface of the specimens under given normal forces, with the overarching goal to observe the change of friction force with respect to normal force. The defined areas were first carefully cleaned by mechanical cleaning with another LFM tip under 20nN to eliminate remaining residual during transfer process. Topographic images with cross-sectional profiles and FFM images with friction loops of measured areas on bi-layer MoS₂ on CNT matrix under various CNT density are shown in Figure 3.2 a,b, respectively. On the basis of the FFM data, significant changes in friction were observed at the areas with different CNT density. The higher the applied load, the higher friction force on these specimens. The elasticity of carbon nanotubes (CNTs) has been shown to have a significant impact on the friction and wear behavior of two-dimensional (2D) materials. CNTs are known for their high mechanical strength and flexibility, which can play a crucial role in reducing friction and wear between two surfaces in contact.

The elasticity of carbon nanotubes (CNTs) can affect the friction and wear of two-dimensional (2D) materials in several ways. The elasticity of CNTs can influence the contact

mechanics between the CNT and the 2D material, leading to changes in the friction and wear behavior. If the CNTs are highly elastic, they may deform under the applied load, leading to a reduction in the effective contact area and a corresponding decrease in the friction force. When a 2D material supported with CNTs is subjected to friction and wear, the CNTs can bend and deform under the stress of the sliding motion. This deformation can help to dissipate the energy generated by the friction and wear process, reducing the overall wear rate of the 2D material. Furthermore, the high mechanical strength of CNTs can also help to prevent the formation of cracks or other defects in the 2D material, which can also contribute to reduced wear and friction. The elasticity of CNTs can impact the adhesion between the CNT and the 2D material, which can affect both the friction and wear behavior. If the CNTs are highly elastic, they may not form a strong enough bond with the 2D material, leading to a higher likelihood of sliding and wear. The elasticity of CNTs can impact the sliding behavior of the 2D material. If the CNTs are highly elastic, they may be able to better conform to the surface of the 2D material, reducing the sliding friction. Conversely, if the CNTs are stiff, they may cause increased friction by acting as obstacles to the sliding motion.

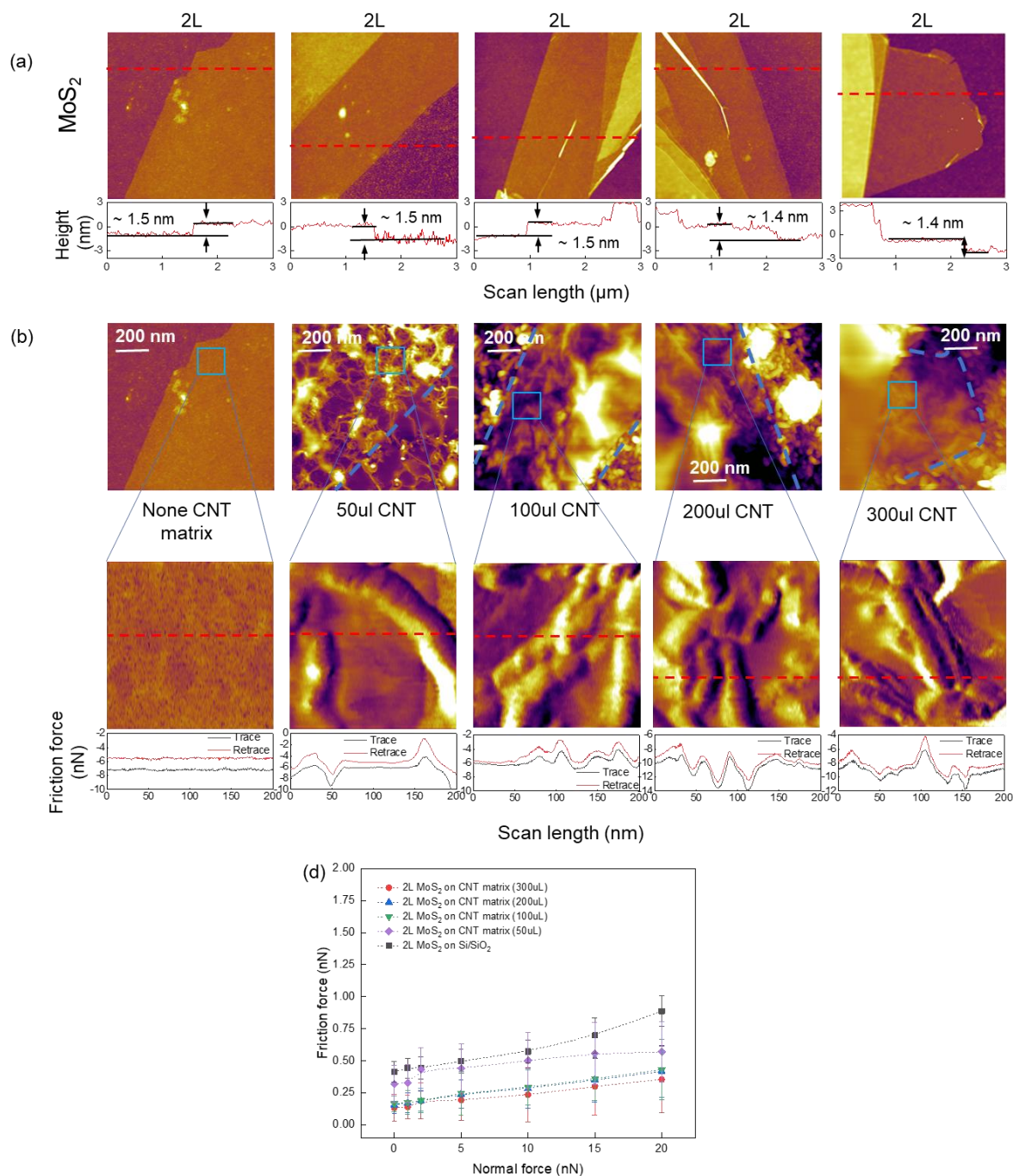


Figure 3. 2 Friction force as a function of normal force with different E of CNT matrix with a MoS₂ thickness of 2L (~ 1.5nm). (a) AFM topographic images of MoS₂ before and after transferring onto CNT matrix (b) FFM (forward scan) images of MoS₂ at 20nN normal force. (c) variations in friction force of the MoS₂ on CNT matrix and Si/SiO₂ for 2L with respect to the normal force. In (a)-(b), the red dashed lines indicate the locations where the cross-sectional profiles, and friction loops were taken.

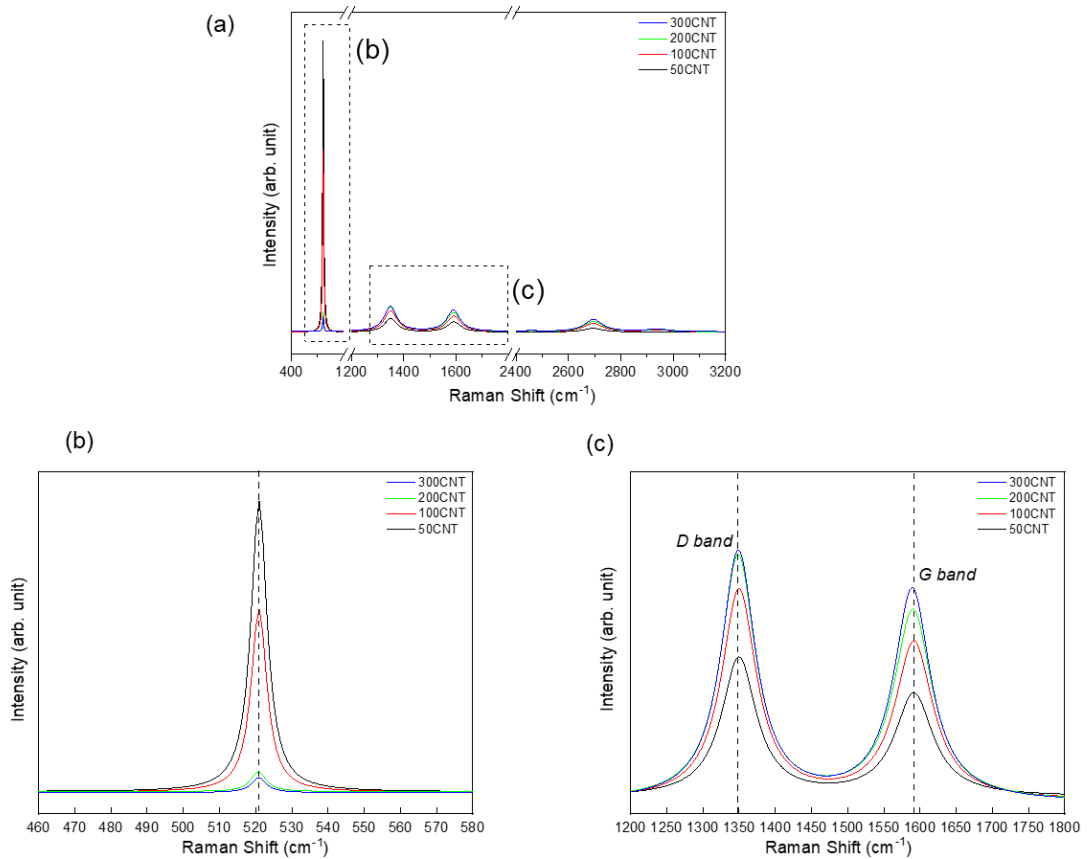


Figure 3. 3 (a) Raman spectra of the studied samples obtained at room temperature using 532 nm wavelength laser. (b) Raman spectrum of Si/SiO₂ of 4 specimens. The inset (c) shows the Raman spectrum of CNT on Si/SiO₂ substrate obtained at room temperature with the same laser excitation.

One key observation is that a higher density of CNTs in a matrix can result in a higher Raman peak intensity of CNT compared to a lower density in Figure 3.3 c. This is due to the increased likelihood of Raman scattering events occurring as more CNTs are present in the sample. The higher density also leads to stronger CNT-CNT interactions, which can influence the Raman spectrum through changes in the CNTs' vibrational modes. This observation suggests that the CNT matrix on the Si substrate has a different thickness. It is hypothesized that the thicker CNT matrix could induce stress and strain on the Si substrate, leading to changes in the Si's Raman spectrum. Additionally, the thicker CNT matrix may reduce the Si's exposure to

incident laser light, further contributing to the lower Raman intensity in Figure 3.3 b. These findings highlight the importance of understanding the effect of CNT density on the Raman spectra of both the CNTs and the other materials in the matrix, as it can provide insights into the underlying physics and potential applications of CNT-based materials.

In this study, we investigated the effect of elasticity on the friction force of a carbon nanotube (CNT) matrix. Our results show that the elasticity of the CNT matrix plays a significant role in determining its friction properties. Specifically, we found that a more elastic CNT matrix exhibits a lower friction force compared to a less elastic one. This can be attributed to the fact that a more elastic matrix is better able to conform to the surface it is in contact with, resulting in less resistance to sliding. Additionally, we observed that the elasticity of the matrix had minimal effect on the density of the CNTs post-transfer, suggesting that the transfer process did not compromise the structural integrity of the matrix.

3.3. The effect of suspended MoS₂

The behavior of supported and suspended graphene and MoS₂ can be quite different due to their unique properties and interactions with substrates. Supported graphene tends to have higher friction compared to suspended graphene due to increased adhesion and surface roughness caused by the substrate. On the other hand, supported MoS₂ can have lower friction compared to suspended MoS₂ due to the smoother surface caused by the substrate. This contrasting behavior highlights the importance of studying the frictional behavior of 2D materials in different configurations. In particular, further investigation into the friction of suspended MoS₂ on carbon nanotubes (CNTs) can provide insights into the effect of suspension on the frictional behavior of MoS₂ and its potential applications in nanotribology. This research can also lead to a better understanding of the underlying mechanisms that govern wear resistance and lubrication of MoS₂ on CNT matrix.

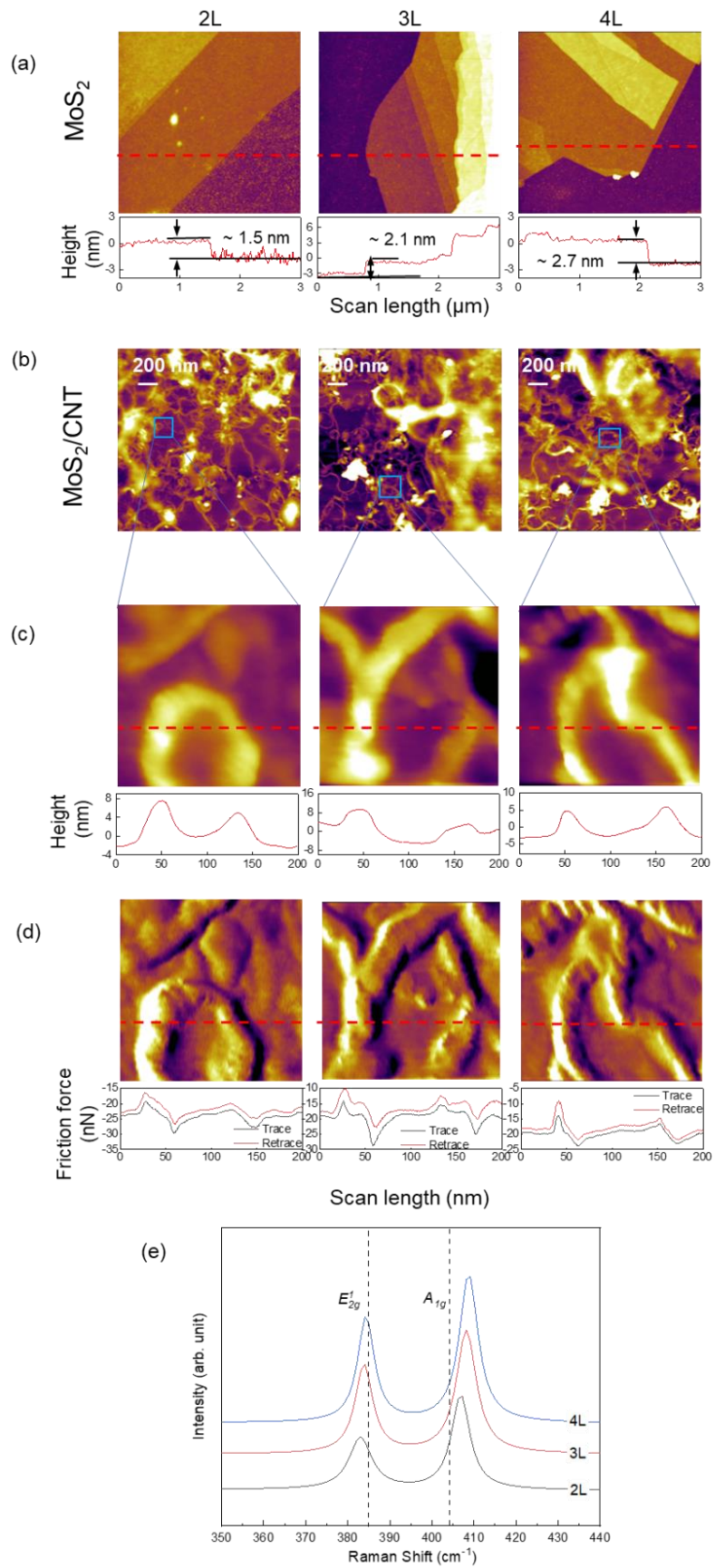


Figure 3. 4 Friction force as a function of normal force with different suspended MoS₂ thickness (a) (b) AFM topographic images of MoS₂ before and after transferring onto CNT matrix (c) FFM (forward scan) images of suspended MoS₂ on CNT fiber at 20nN normal force. The inset (c) shows the topography images of measured areas. Raman spectra and E_{2g}¹ and A_{1g}. In (a)-(c)-(d), the red dashed lines indicate the locations where the cross-sectional profiles, and friction loops were taken.

Figure 6a shows topographic images of exfoliated MoS₂ before the transfer and Figures 3.4 b shows the topographic images of MoS₂ after the transfer onto the CNT matrix. Figure 6c shows the AFM images of mono, bi, and tri layer MoS₂ nanoflake suspended on the CNT fiber. Parts d of Figure 3.4 show the friction images of suspended MoS₂. Apparently, the friction on the suspended MoS₂ is much larger than that on the supported MoS₂. This can be attributed to the smaller out-of-plane bending stiffness and easier puckering tendency on the suspended MoS₂. [48,49]

The friction on the suspended and supported MoS₂ nanoflake with different thickness is shown in Figure 3.4a. The Raman spectra frequency differences (E_{2g}¹ and A_{1g}) of the MoS₂ nanoflake with different layers are shown in Figure 3.4 e. For the MoS₂ supported on the SiO₂/Si substrate, the friction force decreases with the increasing layer numbers. This is in good agreement with previous works, and it is attributed to the puckering effect. [50] For the suspended MoS₂ nanoflake, the friction force shows a similar thickness dependence.

This can be attributed to the interface effect, mainly the underlying interaction strength between the MoS₂ nanoflake and the substrate that affects the friction. The probe on the suspended MoS₂ is more apt to generate puckering and surface fluctuations because of the reduced bending rigidity without the substrate supporting. [51] The friction force on the suspended MoS₂ decreases with the increasing layer numbers in Figure 3.4. In previous research, the friction on the suspended graphene membrane decreased with increasing load in the positive load regime and behaved a switch during the near zero load region, and this can be

attributed to the effect of adhesion force.[52] This phenomenon is to the contrary of our result that the friction on the suspended MoS₂ increases with the applied load. The explanation for this is that the applied load in our experiments is much larger than that in the literature and it can overcome the adverse influence of the adhesion force between the tip and the MoS₂ nanoflake.

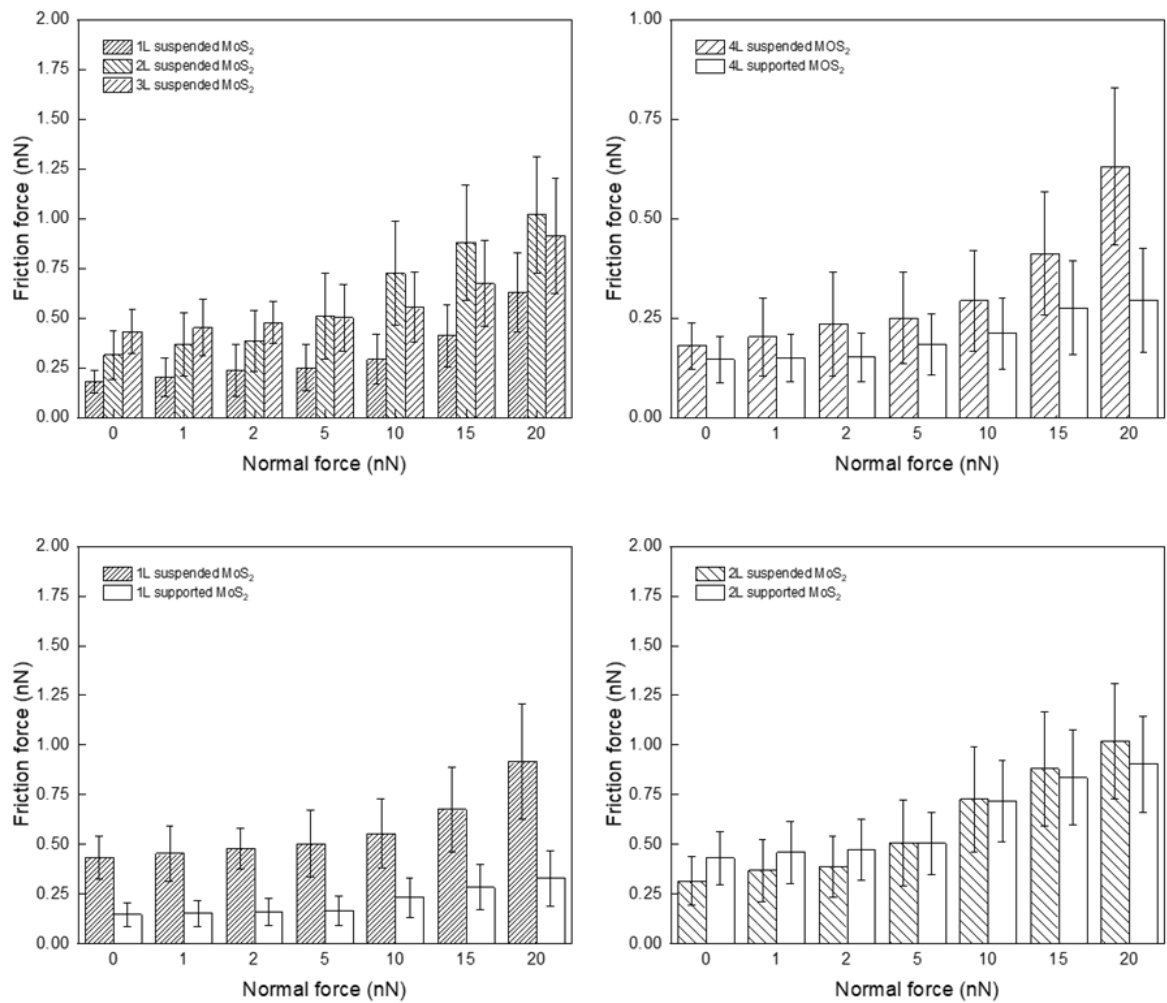


Figure 3. 5 Frictional forces for suspended MoS₂ on CNT for 2L, 3L, 4L MoS₂ with respect to the normal force.

3.4. The effect of MoS₂ thickness

It has been proposed that multilayer MoS₂ provides better tribological characteristics than single-layer MoS₂. [53] However, the mechanism for this enhancement has not yet been clearly explained in conjunction with CNT matrix. To elucidate this mechanism, we investigate the friction force of MoS₂ on CNT matrix. The friction force variation with respect to MoS₂ layer thickness and the corresponding topographic and FFM images of defined areas for number of MoS₂ layer are shown in Figures 3.6 a,b respectively.

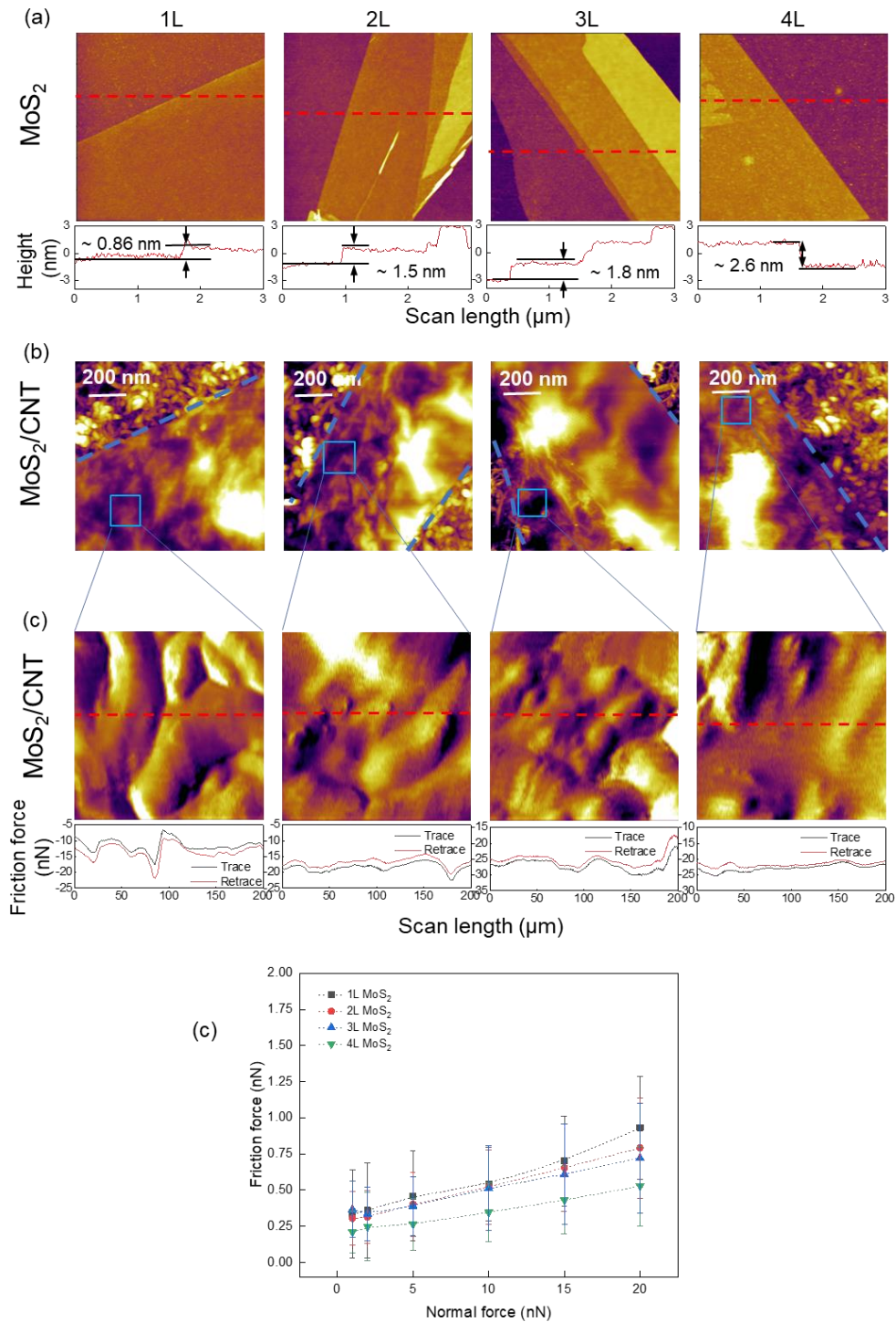


Figure 3. 6 (a) AFM topographic images, (b) FFM (forward scan) images of MoS₂ at 20nN normal force, and (c) variations in friction force of the MoS₂ on CNT matrix for 1L, 2L, 3L, 4L MoS₂ with respect to the normal force. In (a)-(b), the red dashed lines indicate the locations where the cross-sectional profiles, and friction loops were taken.

The friction forces from the friction tests are plotted with respect to the number of layers in Figure 3.6 c, which clearly shows thickness-dependent friction behavior for MoS₂. At the same normal force, friction force was found to increase as the number of layers decreased, resulting in the largest friction for single-layer specimens. The dependence of friction force on the number of layers is a general trend for these layered materials and has been attributed to the out-of-plane deformation or “puckering” of the top layers in front of the AFM tip during contact sliding.

The decrease in friction with an increasing number of layers of MoS₂ can be attributed to its layered structure. MoS₂ is a two-dimensional (2D) material composed of layers of molybdenum and sulfur atoms. The layers are held together by weak van der Waals forces, which allows for easy sliding between the layers. As the number of layers increases, the total surface area of the material also increases, which leads to an increase in the number of van der Waals interactions between the layers. These interactions act to stabilize the layers, making it more difficult for them to slide against each other. The effect of increased van der Waals interactions is offset by a decrease in the number of structural defects, such as grain boundaries, that can act as sites for energy dissipation and friction. In other words, as the number of layers increases, the overall quality of the material improves, leading to a reduction in friction. The decrease in friction with an increasing number of layers of MoS₂ is due to the combination of increased van der Waals interactions and improved material quality.

3.5. The effect of CNT orientation

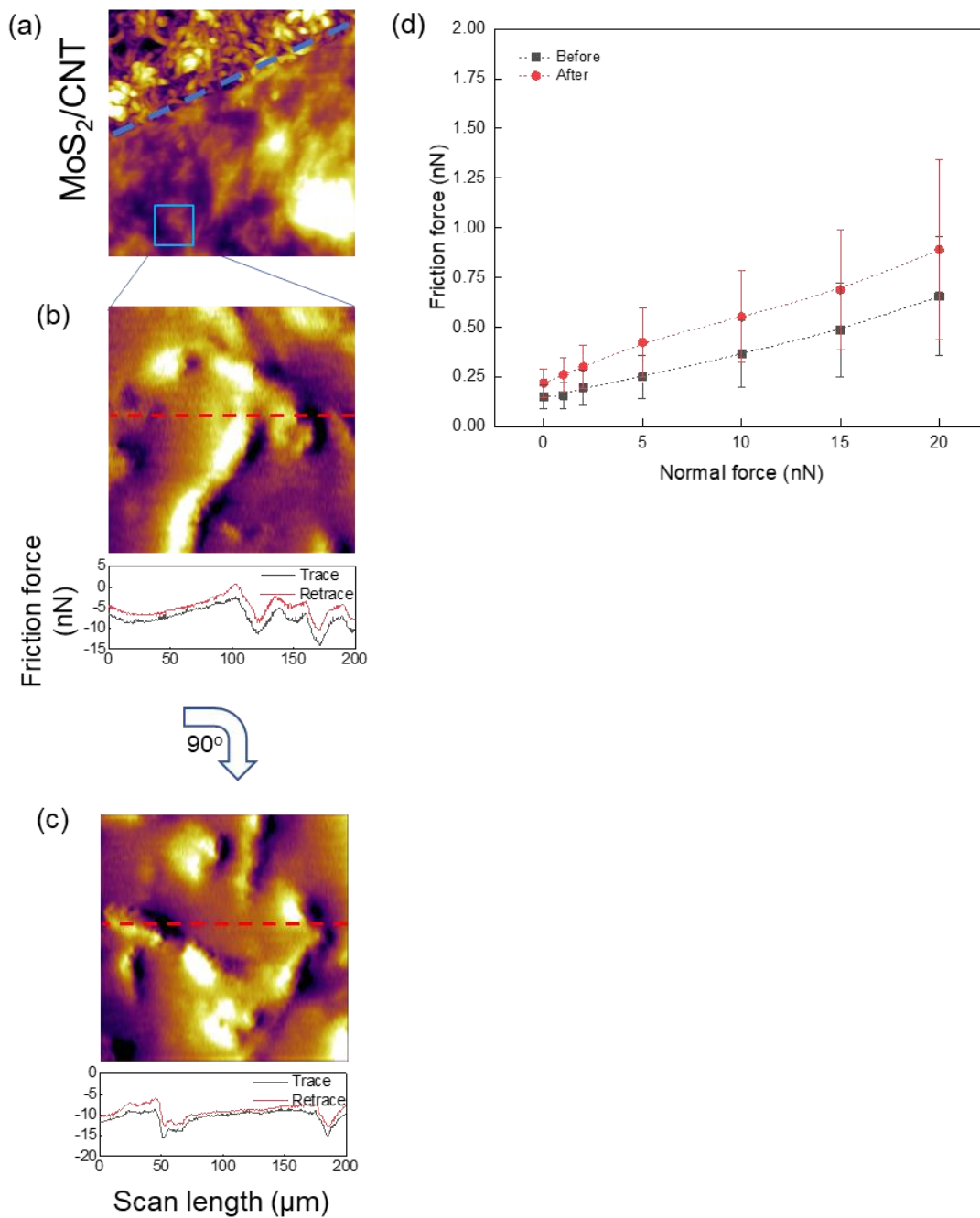


Figure 3. 7 (a) AFM topographic images of MoS₂ onto CNT matrix. Friction images of the normal orientation (b) and after rotating the specimen of 90 degrees (c). (d) variations in friction force of the MoS₂ on CNT matrix for different sliding motion with respect to the normal force. The red dashed lines indicate the locations where the cross-

sectional profiles, and friction loops were taken. The friction force profile (red solid line) is the average profile inside the area delimited by the dotted line in b,c.

We utilized atomic force microscopy (AFM) and friction force microscopy (FFM) to obtain friction results and AFM images. The findings proposed a CNT orientation-related friction force, which was shown in Figure 3.7, indicating that the friction force of MoS₂/CNT sliding in the normal orientation was higher compared to the later one after rotating the specimen of 90 degrees. The study hypothesizes that the higher friction force observed in the normal orientation may be contributed to the aligned CNTs below the MoS₂ layer. When the sliding direction is perpendicular to the orientation of the CNTs, the friction force is typically lower compared to when the sliding direction is parallel to the CNTs. [54, 55] This difference in friction force can be attributed to the change in contact area between the MoS₂ layer and the CNTs. A higher CNT density can provide more anchoring points for MoS₂ layers, leading to a higher friction force. On the other hand, a lower density may allow MoS₂ layers to slip more easily, resulting in a lower friction force. Overall, the density and orientation of the CNT matrix can influence the friction force of MoS₂ on the surface, leading to variations in friction force depending on the direction of the sliding motion. The study highlights the importance of investigating the underlying mechanisms responsible for these effects. The results provide valuable insights into the complex interactions between MoS₂ and CNTs and their effect on the friction force.

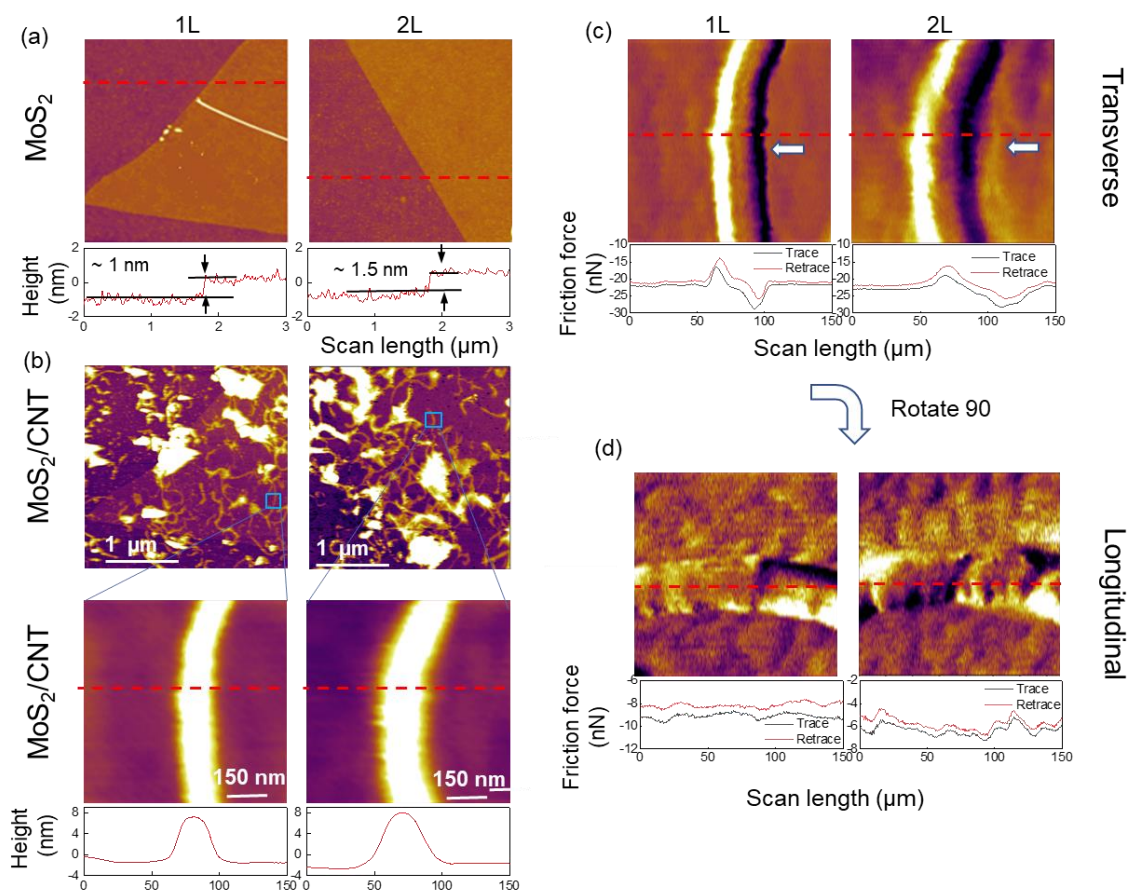
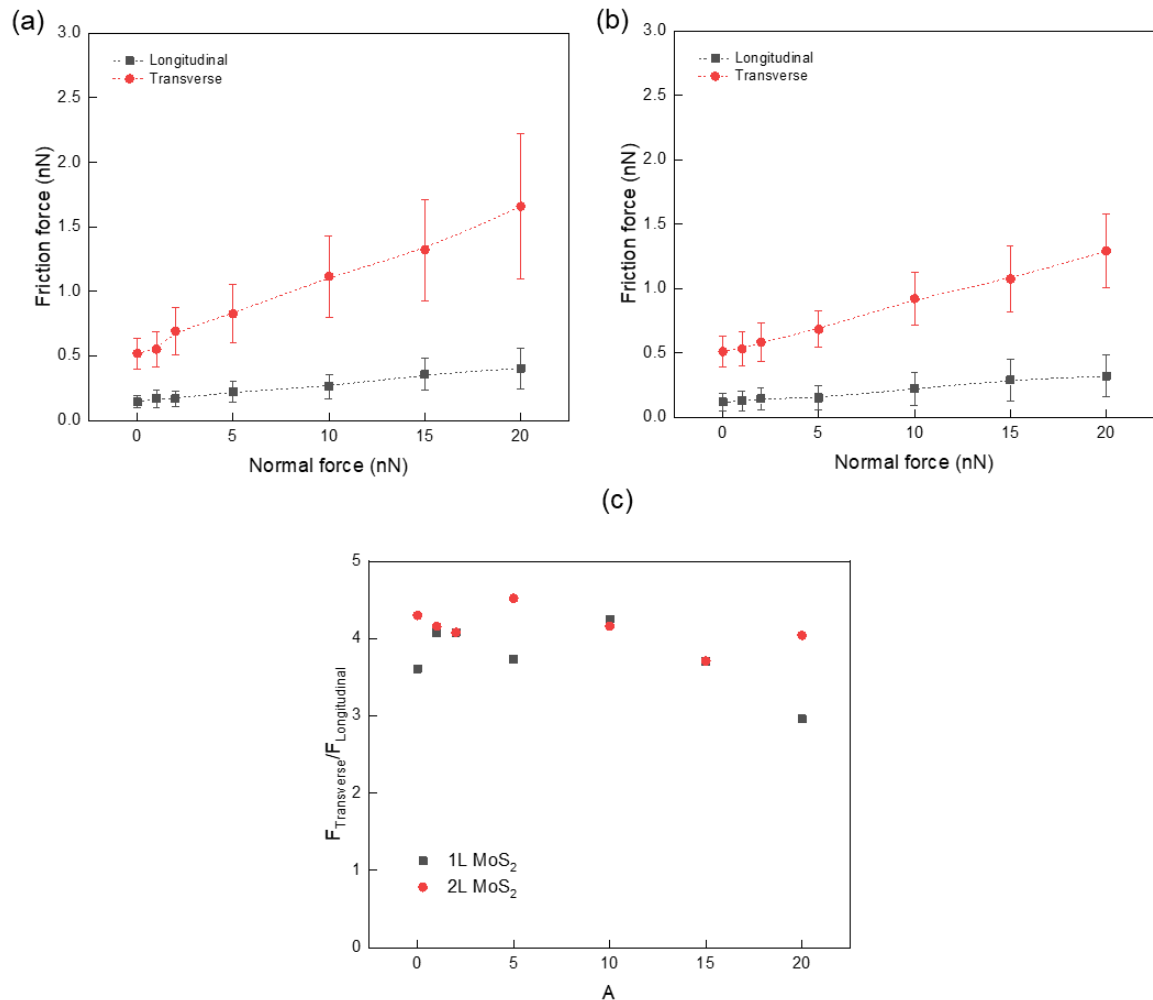


Figure 3. 8 (a),(b) AFM topographic images of MoS₂ before and after transferring onto CNT matrix. Friction images of the highlighted transverse (c) and longitudinal (d). The red dashed lines indicate the locations where the cross-sectional profiles, and friction loops were taken. The friction force profile (red solid line) is the average profile inside the area delimited by the dotted line in c,d.

The MoS₂/CNTs used in this study are deposited on a flat silicon substrate by spin coating and transfer process. The topography and friction properties of the MoS₂ on CNTs fiber were characterized by AFM. To measure the transverse and longitudinal friction force on a nanotube, we looked for an isolated of CNTs on the silicon surface and we took simultaneous topographical and frictional images in different MoS₂ layers and at the same scales. In Figure 10, we show some examples of MoS₂/CNTs that have been measured. We usually look for

nanotubes that lie on the substrate with some sections parallel and some other sections perpendicular to the tip scan direction. We then zoom into the desired section and we acquire a friction and topography image (Figure 3.8 b,c). Typical cross-sections of the friction and



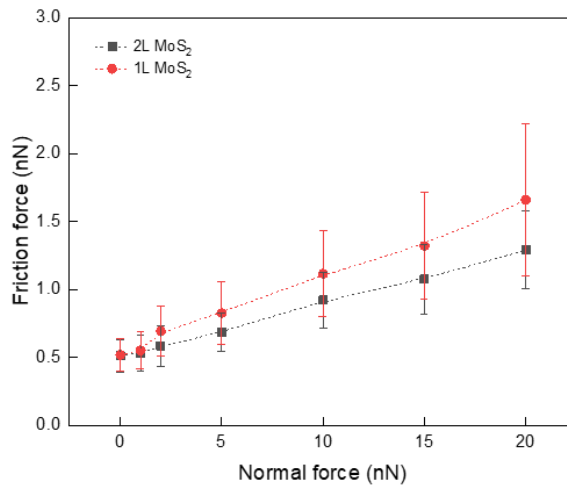
topography images for longitudinal and transverse measurements are shown in Figure 10b,c.

Figure 3. 9 (a)-(c) Anisotropy ratio of friction on MoS₂ with different thicknesses. (d) The friction ratio as a function of normal load on MoS₂ different thicknesses.

A comparison of the friction force of MoS₂ on CNT fibers between 1-layer (1L) and 2-layer (2L) MoS₂ reveals interesting insights. Research studies have shown that the friction force between MoS₂ and CNT fibers differs depending on the thickness of MoS₂, with 2L MoS₂ exhibiting a smaller friction force compared to 1L MoS₂. The number of layers in MoS₂ has

been found to play a significant role in the friction behavior. The reduced friction force observed for 2L MoS₂ on CNT fibers can be attributed to the interlayer interactions between the MoS₂ layers, which can result in a more slippery surface compared to the single-layer MoS₂. Additionally, the presence of additional layers in 2L MoS₂ can lead to increased spacing between the layers, reducing the van der Waals forces between MoS₂ and the CNT fibers. This can result in a lower friction force as the interfacial interactions are weakened. Further studies are needed to elucidate the underlying mechanisms responsible for the observed differences in friction behavior between 1L and 2L MoS₂ on CNT fibers, but these findings highlight the influence of MoS₂ thickness on the friction characteristics of MoS₂/CNT interfaces. Further studies on the friction behavior of MoS₂ on CNT fibers with different MoS₂ thicknesses will help uncover the intricate interplay between the number of layers in MoS₂ and the resulting friction properties, leading to the development of advanced tribological systems with enhanced performance and durability.

Transverse direction



Longitudinal direction

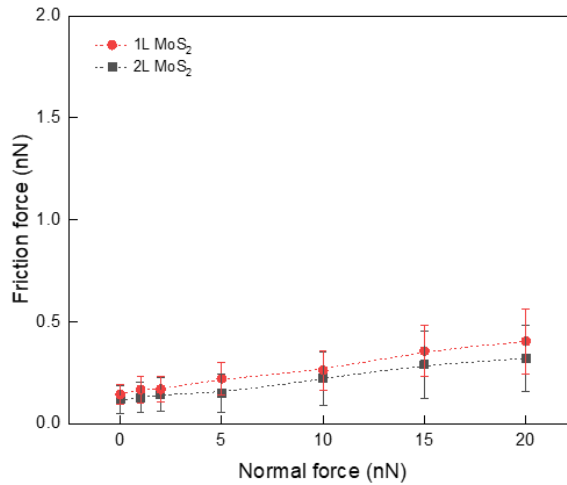


Figure 3. 10. Frictional forces for transverse and longitudinal sliding

In Figure 3.10 a and b, the corresponding transverse friction forces and longitudinal friction forces as a function of normal loads are shown. As consistently observed in our experiments, it is evident that the friction force is larger for 1L MoS₂/CNT and smaller for 2L MoS₂/CNT in both sliding directions.

The sliding direction of the motion plays a crucial role in the friction behavior of MoS₂ on CNT fiber. The transverse friction force and longitudinal friction force measurements provide insights into the friction behavior in two different directions. The transverse direction is

perpendicular to the CNT alignment, while the longitudinal direction is parallel to the CNT alignment. The differences in friction forces in these two directions may be attributed to the orientation-dependent interfacial interactions between MoS₂ and CNTs. In the case of 1L MoS₂/CNT, the higher friction force in both directions could be related to the alignment of CNTs, while the lower friction force in 2L MoS₂/CNT may indicate reduced interfacial interactions in both directions due to differences in layer arrangement and CNT alignment.

The friction in the longitudinal direction of a carbon nanotube (CNT) is higher than in the transverse direction due to the unique structure and bonding of CNTs.

In the longitudinal direction, the carbon atoms are tightly packed in a spiral arrangement and are held together by strong covalent bonds. This results in a high density of chemical bonds along the axis of the CNT, which results in stronger van der Waals interactions with the surface in contact. This leads to a higher friction force in the longitudinal direction.

In the transverse direction, the arrangement of carbon atoms is more open, and the covalent bonds are weaker. This results in fewer chemical bonds and weaker van der Waals interactions with the surface, leading to a lower friction force in the transverse direction.

The friction anisotropy of CNTs is due to the cylindrical shape and the arrangement of the carbon atoms, which results in a higher friction force in the longitudinal direction and a lower friction force in the transverse direction.^{24,25}

The frictional properties of CNTs can also be influenced by other factors, such as the type of surface in contact, the environmental conditions, and the mechanical loading conditions. For example, the frictional behavior of CNTs can be influenced by the presence of contaminants on the surface, the temperature and humidity of the environment, and the applied load and sliding velocity.

The comparison between 1L and 2L MoS₂ on CNT fiber reveals that the number of MoS₂ layers can impact the friction behavior, with 2L MoS₂ exhibiting lower friction compared to

1L MoS₂. The differences in friction forces in transverse and longitudinal directions suggest that the orientation of CNTs and the interfacial interactions between MoS₂ and CNTs are critical factors affecting the friction behavior of MoS₂ on CNT fiber.

4. CONCLUSIONS AND RECOMMENDATIONS

4.1. Conclusions

In this research, the friction characteristics of MoS₂ on CNT have been investigated. CNT effect on friction characteristics of MoS₂ specimens has been systematically studied. The objective of this work was first to contribute to the scientific understanding of the tribological behavior of MoS₂/CNT for improved friction resistance and lubrication to gain a better understanding of the relationship between CNT and tribological performance in these materials. Specifically, the aim is to identify how changes in the density of CNT impact the friction behavior of MoS₂/CNT and to investigate the underlying mechanisms responsible for these effects. To do this, the AFM-based approaches and surface analyses using various microscopy systems were conducted. Based on these approaches regarding the several effects, the following conclusions were drawn:

1. Quantitatively friction force measurement on supported MoS₂ onto PMMA, CNT matrix, and Si/SiO₂ was conducted. Our study found that the friction coefficient of MoS₂ on the CNT matrix was lower than that on PMMA and Si/SiO₂, with values of 0.22, 0.33, and 0.17, respectively under 2nN. This suggests that the use of a CNT matrix as a substrate may be advantageous in certain applications where a lower friction coefficient is desired.
2. The density of the CNT effect on the friction of these MoS₂/CNT specimens including different CNT densities was investigated. Through the transfer process, we observed that the density of the matrix had minimal effect on the density of the CNTs post-transfer. Furthermore, significant changes in friction were observed in the areas with different CNT densities. A more elastic CNT matrix exhibits a lower friction force compared to a less elastic one. The higher the applied load, the higher the friction force on these specimens.
3. The effect of suspended MoS₂ specimens on CNT fiber was also investigated quantitatively. Supported MoS₂ tends to have lower friction compared to suspended MoS₂ due

to the smoother surface caused by the substrate. This contrasting behavior highlights the importance of studying the frictional behavior of 2D materials in different configurations. Moreover, for the MoS₂ supported on the SiO₂/Si substrate, the friction force decreases with the increasing layer numbers. This is in good agreement with previous works and it is attributed to the puckering effect. For the suspended MoS₂ nanoflake, the friction force shows a similar thickness dependence.

4. The effect of the number of MoS₂ layers on the friction of these MoS₂/CNT specimens including 1L to 4L MoS₂ was investigated. At the same normal force, friction force was found to increase as the number of layers decreased, resulting in the largest friction for single-layer specimens. The dependence of friction force on the number of layers is a general trend for these layered materials and has been attributed to the out-of-plane deformation or “puckering” of the top layers in front of the AFM tip during contact sliding.

5. Anisotropic friction on MoS₂/CNT was also observed, The friction in the longitudinal direction of a carbon nanotube (CNT) is higher than in the transverse direction due to the unique structure and bonding of CNTs. The differences in friction forces in transverse and longitudinal directions suggest that the orientation of CNTs and the interfacial interactions between MoS₂ and CNTs are critical factors affecting the friction behavior of MoS₂ on CNT fiber.

4.2. Recommendation for future works

1. Exploration of other 2D materials: Although MoS₂ has been extensively studied for its tribological properties, there are other 2D materials that have shown promising properties for tribological applications. Future research should explore the tribological performance of other 2D materials, such as Graphene and h-BN, when combined with MWCNTs.

2. Examination of MWCNTs orientation: The orientation of MWCNTs in the 2D materials matrix can also affect the tribological performance of the composite. Future research should investigate the effect of MWCNTs orientation on the tribological properties by aligned CNT.

3. Exploration of the interfacial properties and surface damage characteristics of other 2D materials when supported on a CNT matrix: While h-BN, MoS₂, and graphene are the most commonly studied 2D materials, there are other 2D materials that may show better interfacial strength and surface damage characteristics when supported on a CNT matrix. Future research should explore the interfacial properties and surface damage characteristics of other 2D materials when supported on a CNT matrix.

4. Investigation of different types of CNTs: The effect of different types of CNTs on the interfacial strength and surface damage characteristics of atomically thin 2D materials should be studied. Different types of CNTs, such as single-walled CNTs and multi-walled CNTs, may have different interfacial properties with the 2D materials and may affect the surface damage characteristics differently.

REFERENCES

- [1] K.S. Novoselov, Nobel Lecture: Graphene: Materials in the Flatland, *Rev.Mod.Phys.* 83 (2011), pp. 837-849.
- [2] K.S. Novoselov, A.K. Geim, S.V. Morozov, D. Jiang, Y. Zhang, S.V. Dubonos, I.V. Grigorieva and A.A. Firsov, Electric Field Effect in Atomically Thin Carbon Films, *Science.* 306 (2004), pp. 666-669.
- [3] V. Singh, D. Joung, L. Zhai, S. Das, S.I. Khondaker and S. Seal, Graphene Based Materials: Past, Present and Future, *Progress in Materials Science.* 56 (2011), pp. 1178-1271.
- [4] M. Taghioskoui, Trends in Graphene Research, *Materials Today.* 12 (2009), pp. 34-37.
- [5] P. Avouris and C. Dimitrakopoulos, Graphene: Synthesis and Applications, *Materials Today.* 15 (2012), pp. 86-97.
- [6] D. Lembke and A. Kis, Breakdown of High-Performance Monolayer MoS₂ Transistors, *ACS Nano.* 6 (2012), pp. 10070-10075.
- [7] A. Kuc, N. Zibouche and T. Heine, Influence of Quantum Confinement on the Electronic Structure of the Transition Metal Sulfide TS₂, *Phys.Rev.B.* 83 (2011), pp. 245213.
- [8] Radisavljevic, B. Radenovic, A. Brivio, J. Giacometti, V. Kis, A., Single-Layer MoS₂ Transistors, *Nat Nano.* 6 (2011), pp. 147-150.
- [9] B. Radisavljevic, M.B. Whitwick and A. Kis, Integrated Circuits and Logic Operations Based on Single-Layer MoS₂, *ACS Nano.* 5 (2011), pp. 9934-9938.
- [10] Z. Yin, H. Li, H. Li, L. Jiang, Y. Shi, Y. Sun, G. Lu, Q. Zhang, X. Chen and H. Zhang, Single-Layer MoS₂ Phototransistors, *ACS Nano.* 6 (2012), pp. 74-80.

[11] H.S. Lee, S. Min, Y. Chang, M.K. Park, T. Nam, H. Kim, J.H. Kim, S. Ryu and S. Im, MoS₂ Nanosheet Phototransistors with Thickness-Modulated Optical Energy Gap, *Nano Lett.* 12 (2012), pp. 3695-3700.

[12] H. Li, Z. Yin, Q. He, H. Li, X. Huang, G. Lu, D.W.H. Fam, A.I.Y. Tok, Q. Zhang and H. Zhang, Fabrication of Single- and Multilayer MoS₂ Film-Based Field-Effect Transistors for Sensing NO at Room Temperature, *Small.* 8 (2012), pp. 63-67.

[13] F.K. Perkins, - Chemical Vapor Sensing with Monolayer MoS₂, - *Nano Lett.* 13 (2013), pp. 2013/02/13.

[14] S. Bertolazzi, J. Brivio and A. Kis, Stretching and Breaking of Ultrathin MoS₂, *ACS Nano.* 5 (2011), pp. 9703-9709.

[15] A. Castellanos-Gomez, M. Poot, G.A. Steele, H.S.J. van der Zant, N. Agrait and G. Rubio-Bollinger, Elastic Properties of Freely Suspended MoS₂ Nanosheets, *Adv Mater.* 24 (2012), pp. 772-775.

[16] B. Windom, W.G. Sawyer and D. Hahn, A Raman Spectroscopic Study of MoS₂ and MoO₃: Applications to Tribological Systems, *Tribology Letters.* 42 (2011), pp. 301-310.

[17] C. Lee, Q. Li, W. Kalb, X. Liu, H. Berger, R.W. Carpick and J. Hone, Frictional Characteristics of Atomically Thin Sheets, *Science.* 328 (2010), pp. 76-80.

[18] J.S. Choi, J. Kim, I. Byun, D.H. Lee, M.J. Lee, B.H. Park, C. Lee, D. Yoon, H. Cheong, K.H. Lee, Y. Son, J.Y. Park and M. Salmeron, Friction Anisotropy-Driven Domain Imaging on Exfoliated Monolayer Graphene, *Science.* 333 (2011), pp. 607-610.

[19] L. Lin, D. Kim, W. Kim and S. Jun, Friction and Wear Characteristics of Multi-Layer Graphene Films Investigated by Atomic Force Microscopy, *Surface and Coatings Technology.* 205 (2011), pp. 4864-4869.

[20] S. Kwon, J. Ko, K. Jeon, Y. Kim and J.Y. Park, Enhanced Nanoscale Friction on Fluorinated Graphene, *Nano Lett.* 12 (2012), pp. 6043-6048.

[21] D. Cho, L. Wang, J. Kim, G. Lee, E.S. Kim, S. Lee, S.Y. Lee, J. Hone and C. Lee, Effect of Surface Morphology on Friction of Graphene on various Substrates, *Nanoscale.* 5 (2013), pp. 3063-3069.

[22] S. Najmaei, Z. Liu, P.M. Ajayan and J. Lou, Thermal Effects on the Characteristic Raman Spectrum of Molybdenum Disulfide (MoS_2) of Varying Thicknesses, *Appl.Phys.Lett.* 100 (2012), pp. 013106.

[23] A. Castellanos-Gomez, M. Barkelid, A.M. Goossens, V.E. Calado, d.Z. van and G.A. Steele, Laser-Thinning of MoS_2 : On Demand Generation of a Single-Layer Semiconductor, *Nano Lett.* 12 (2012), pp. 3187-3192.

[24] G.H. Han, S.J. Chae, E.S. Kim, I.H. Lee, S.W. Lee, S.Y. Lee, S.C. Lim, H.K. Jeong, M.S. Jeong and Y.H. Lee, Laser Thinning for Monolayer Graphene Formation: Heat Sink and Interference Effect, *ACS Nano.* 5 (2011), pp. 263-268.

[25] X. Lu, M.I.B. Utama, J. Zhang, Y. Zhao and Q. Xiong, Layer-by-Layer Thinning of MoS_2 by Thermal Annealing, *Nanoscale.* 5 (2013), pp. 8904-8908.

[26] V.K. Sangwan, H.N. Arnold, D. Jariwala, T.J. Marks, L.J. Lauhon and M.C. Hersam, Low-Frequency Electronic Noise in Single-Layer MoS_2 Transistors, *Nano Lett.* 13 (2013), pp. 4351-4355.

[27] Z.H. Ni, H.M. Wang, J. Kasim, H.M. Fan, T. Yu, Y.H. Wu, Y.P. Feng and Z.X. Shen, Graphene Thickness Determination using Reflection and Contrast Spectroscopy, *Nano Lett.* 7 (2007), pp. 2758-2763.

[28] Lee. C, Yan. H, Brus-Louis. E, Heinz-Tony F, Hone and R.S. J, Anomalous Lattice Vibrations of Single- and Few-Layer MoS_2 , - *ACS Nano.* 4 (2010), pp. 2695-2700.

[29] H. Li, Q. Zhang, C.C.R. Yap, B.K. Tay, T.H.T. Edwin, A. Olivier and D. Baillargeat, From Bulk to Monolayer MoS₂: Evolution of Raman Scattering, *Advanced Functional Materials*. 22 (2012), pp. 1385-1390.

[30] N.A. Lanzillo, A. Glen Birdwell, M. Amani, F.J. Crowne, P.B. Shah, S. Najmaei, Z. Liu, P.M. Ajayan, J. Lou, M. Dubey, S.K. Nayak, O&apos and T.P. Regan, Temperature-Dependent Phonon Shifts in Monolayer MoS₂, *Appl.Phys.Lett.* 103 (2013).

[31] Wang, H., Li, C., Fang, P., Zhang, Z., & Zhang, J.Z. (2018). Synthesis, properties, and optoelectronic applications of two-dimensional MoS₂ and MoS₂-based heterostructures. *Chemical Society reviews*, 47 16, 6101-6127 .

[32] Martins-Júnior, P. A., Alcântara, C. E., Resende, R. R., & Ferreira, A. J. (2013). Carbon nanotubes: directions and perspectives in oral regenerative medicine. *Journal of Dental Research*, 92(7), 575-583

[33] J.L. Hutter and J. Bechhoefer, Calibration of Atomic-force Microscope Tips, *Rev.Sci.Instrum.* 64 (1993), pp. 1868-1873.

[34] M. Varenberg, I. Etsion and G. Halperin, An Improved Wedge Calibration Method for Lateral Force in Atomic Force Microscopy, *Review of Scientific Instruments*. 74 (2003), pp. 3362-3367.

[35] K. Chung, Y. Lee, H. Kim and D. Kim, Fundamental Investigation of the Wear Progression of Silicon Atomic Force Microscope Probes, *Tribology Letters*. 52 (2013), pp. 315-325.

[36] K. Chung, Y. Lee and D. Kim, Characteristics of Fracture during the Approach Process and Wear Mechanism of a Silicon AFM Tip, *Ultramicroscopy*. 102 (2005), pp. 161-171.

[37] B. Gotsmann and M.A. Lantz, Atomistic Wear in a Single Asperity Sliding Contact, *Phys.Rev.Lett.* 101 (2008), pp. 125501.

[38] Madan Sharma; Aditya Singh; and Rajendra Singh. Monolayer MoS₂ Transferred on Arbitrary Substrates for Potential Use in Flexible Electronics. *ACS Applied Nano Materials* 2020 3 (5), 4445-4453.

[39] Kim, G.; Jang, A.-R.; Jeong, H. Y.; Lee, Z.; Kang, D. J.; Shin, H.S. Growth of High-Crystalline, Single-Layer Hexagonal Boron Nitride on Recyclable Platinum Foil. *Nano Lett.* 2013, 13, 1834–1839.

[40] Shearer, C. J.; Slattery, A. D.; Stapleton, A. J.; Shapter, J. G.;Gibson, C. T. Accurate Thickness Measurement of Graphene. *Nanotechnology* 2016, 27, 125704.

[41] Khac, B. C. T.; Jeon, K.-J.; Choi, S. T.; Kim, Y. S.; DelRio, F. W.;Chung, K.-H. Laser-Induced Particle Adsorption on Atomically Thin MoS₂. *ACS Appl. Mater. Interfaces* 2016, 8, 2974–2984.

[42] Gorbachev, R. V.; Riaz, I.; Nair, R. R.; Jalil, R.; Britnell, L.; Belle, B. D.; Hill, E. W.; Novoselov, K. S.; Watanabe, K.; Taniguchi, T.; Geim, A. K.; Blake, P. Hunting for Monolayer Boron Nitride: Optical and Raman Signatures. *Small* 2011, 7, 465–468.

[43] Li, H.; Zhang, Q.; Yap, C. C. R.; Tay, B. K.; Edwin, T. H. T.; Olivier, A.; Baillargeat, D. From Bulk to Monolayer MoS₂: Evolution of Raman Scattering. *Adv. Funct. Mater.* 2012, 22, 1385–1390.

[45] Ferrari, A. C.; Meyer, J. C.; Scardaci, V.; Casiraghi, C.; Lazzeri, M.; Mauri, F.; Piscanec, S.; Jiang, D.; Novoselov, K. S.; Roth, S.; Geim, A. K. Raman Spectrum of Graphene and Graphene Layers. *Phys. Rev. Lett.* 2006, 97, 187401.

[46] Zhi Yang; Bin Dong; Yi Huang; Liang Liu; Feng-Yuan Yan; Hu-Lin Li. A study on carbon nanotubes reinforced poly(methyl methacrylate) nanocomposites. *Materials Letters*. 59, 17,2005, 2128-2132.

[47] Schumacher, A; and Kruse, N; and Prins, R; and Meyer, E; and Luthi, R; and Howald, L; and Guntherodt, H; J. and Scandella, L. Influence of humidity on friction measurements of supported MoS₂ single layers. *Journal of vacuum science & technology. B, Microelectronics and nanometer structures processing, measurement, and phenomena*. 14, 2. 1264-1267.

[48] Quereda, J.; Castellanos-Gomez, A.; Agrait, N.; Rubio-Bollinger, G. Single-layer MoS₂ Roughness and Sliding Friction Quenching by Interaction with Atomically Flat Substrates. *Appl. Phys. Lett.* 2014, 105, No. 053111

[49] Zhang, Y.; Dong, M.; Gueye, B.; Ni, Z.; Wang, Y.; Chen, Y. Temperature Effects on the Friction Characteristics of Graphene. *Appl. Phys. Lett.* 2015, 107, No. 011601.

[50] Lee, C.; Li, Q.; Kalb, W.; Liu, X.; Berger, H.; Carpick, R. W.; Hone, J. Frictional Characteristics of Atomically Thin Sheets. *Science* 2010, 328 (5974), 76–80.

[51] Zhang, Y.; Dong, M.; Gueye, B.; Ni, Z.; Wang, Y.; Chen, Y. Temperature Effects on the Friction Characteristics of Graphene. *Appl. Phys. Lett.* 2015, 107, No. 011601.

[52] Deng, Z.; Klimov, N. N.; Solares, S. D.; Li, T.; Xu, H.; Cannara, R. J. Nanoscale Interfacial Friction and Adhesion on Supported versus Suspended Monolayer and Multilayer Graphene. *Langmuir* 2013, 29 (1), 235–243.

[53] Vasić, B.; Matković, A.; Ralević, U.; Belić, M.; Gajić, R. Nanoscale Wear of Graphene and Wear Protection by Graphene. *Carbon* 2017, 120, 137–144.

[54] Lucas, M., Zhang, X., Palaci, I. et al. Hindered rolling and friction anisotropy in supported carbon nanotubes. *Nature Mater* 8, 876–881.

[55] Chiu HC, Ritz B, Kim S, Tosatti E, Klinke C, Riedo E. Sliding on a nanotube: interplay of friction, deformations and structure. *Adv Mater.* 2012,5,24(21),2879-84.